As release under the microbial sulfate reduction during redox oscillations in the upper Mekong delta aquifers, Vietnam: A mechanistic study

Van T.H. Phan [a,b,*], Rizlan Bernier-Latmani [c], Delphine Tisserand [a], Fabrizio Bardelli [d], Pierre Le Pape [e], Manon Frutschi [c], Antoine Gehin [a], Raoul-Marie Couture [f], Laurent Charlet [a]

[a] University Grenoble Alps, CNRS, IRD, IFSTTAR, Institut des Sciences de la Terre (ISTerre), 38000 Grenoble, France
[b] Ho Chi Minh City University of Technology (HCMUT), Vietnam National University - Ho Chi Minh City (VNU-HCM), 268 Ly Thuong Kiet, District 10, Ho Chi Minh City, Viet Nam
[c] Ecole Polytechnique Fédérale de Lausanne (EPFL), Environmental Microbiology Laboratory (EML), EPFL-ENAC-IIE-EML, Station 6, CH-1015 Lausanne, Switzerland
[d] Institute of Nanotechnology (CNR-Nanotec), 00186 Rome, Italy
[e] Institut de Mineralogie, de Physique des Materiaux et de Cosmochimie (IMPMC), UMR 7590 CNRS-UPMC-IRD-MNHN, 4 place Jussieu, 75252 Paris cedex 05, France
[f] Département de Chimie, Université Laval, 1045 Avenue de la Médecine, Québec, QC G1V 0A6, Canada

HIGHLIGHTS

- Microbial sulfate reduction was found to contribute to arsenic (As) sequestration.
- During anoxic conditions, the conversion of soluble As(V) to As(III) was observed.
- The formation of pyrite, rather than mackinawite was observed in redox cycles.
- Absorption/desorption of aqueous As on Fe-(oxyhydr)oxides and pyrite was observed.

GRAPHICAL ABSTRACT
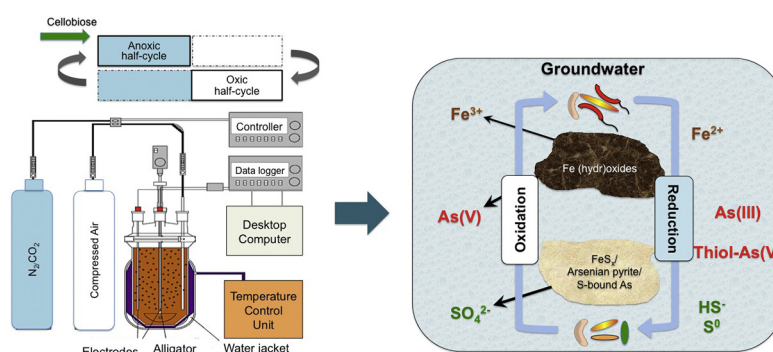
ARTICLE INFO

ABSTRACT

The impact of seasonal fluctuations linked to monsoon and irrigation generates redox oscillations in the subsurface, influencing the release of arsenic (As) in aquifers. Here, the biogeochemical control on As mobility was investigated in batch experiments using redox cycling bioreactors and As- and SO_4^{2-}-amended sediment. Redox potential (E_h) oscillations between anoxic (-300–0 mV) and oxic condition (0–500 mV) were implemented by automatically modulating an admixture of N_2/CO_2 or compressed air. A carbon source (cellobiose, a monomer of cellulose) was added at the beginning of each reducing cycle to stimulate the metabolism of the native microbial community. Results show that successive redox cycles can decrease arsenic mobility by up to 92% during reducing conditions. Anoxic conditions drive mainly the conversion of soluble As(V) to As(III) in contrast to oxic conditions. Phylogenetic analyses of 16S rRNA amplified from the sediments revealed the presence of sulfate and iron – reducing bacteria, confirming that sulfate and iron reduction are key factors for As immobilization from the aqueous phase. As and S K-edge X-ray absorption spectroscopy suggested the association of Fe-(oxyhydr)oxides and the importance of pyrite ($FeS_{2(s)}$), rather than poorly ordered mackinawite ($FeS_{(s)}$), for As sequestration under oxidizing and reducing conditions, respectively. Finally, these findings suggest a role for elemental sulfur in mediating aqueous thioarsenates formation in As-contaminated groundwater of the Mekong delta.

* Corresponding author at: University Grenoble Alps, CNRS, IRD, IFSTTAR, Institut des Sciences de la Terre (ISTerre), 38000 Grenoble, France.
E-mail address: thi-hai-van.phan@univ-grenoble-alpes.fr (V.T.H. Phan).

1. Introduction

Arsenic, a well-known environmental carcinogen, is subject to a variety of mobility-altering processes (WHO IARC, 2004). The World Health Organization's provisional guideline value for total As in drinking water is 10 μg/L. Concentrations of arsenic in groundwater higher than 50 μg/L have been reported in several Southeast Asian countries including Bangladesh, India, Cambodia, China, and Vietnam (e.g. Wang et al., 2018; Van Phan et al., 2017; He and Charlet, 2013; Fendorf et al., 2010; Kocar et al., 2008; van Geen et al., 2008; Zheng et al., 2004; Buschmann et al., 2008). In particular, the Mekong Delta floodplain, which stretches over 62,100 km^2 in Southern Vietnam and South Cambodia, harbors numerous wells with elevated As concentrations (Buschmann et al., 2008; Nguyen et al., 2000). A national survey, conducted by the Department of Water Resources Management monitored the As concentration in tube wells from 2002 to 2008, showed that large areas of the Mekong Delta were contaminated by arsenic, in nearly 900 wells (Erban et al., 2013). Areas with As concentrations in groundwater exceeding 1600 ppb are located along the main Mekong river branches, from An Giang to Can Tho City (Wang et al., 2018; Van Phan et al., 2017; Hanh et al., 2011; Hoang et al., 2010; Nguyen and Itoi, 2009). The origin of As in groundwater of the Mekong Delta is naturally produced by microbial reduction of arsenic-bearing iron oxides in the alluvial sediments (Polya et al., 2005; Rowland et al., 2007; Van Van Dongen et al., 2008; Kocar and Fendorf, 2012; Polizzotto et al., 2008; Stuckey et al., 2015; Winkel et al., 2010). Following river sediment transport, As bound to Fe-(oxyhydr)oxides is delivered to the delta from the Himalayan mountain range. Arsenic is then released to pore water due to the establishment of reducing conditions (Berg et al., 2007; Harvey et al., 2002; Polizzotto et al., 2005; Kocar et al., 2008; Nguyen and Itoi, 2009; Stuckey et al., 2015). Natural organic matter (NOM) supplied from surface sedimentary deposits feeds the dissimilatory reducing bacteria by serving as electron donors that play the important role on As mobilization in this area (Kocar et al., 2008; Lawson et al., 2013; Stuckey et al., 2016; Lawson et al., 2016; Magnone et al., 2017).

In nature, the seasonal reversal of flow direction - rivers to aquifers in the wet season and aquifers to rivers in the dry season - influences the redox balance of the aquifers (Benner et al., 2008; Stuckey et al., 2015). Redox oscillations occurring across the oxic-anoxic interfaces, which are frequent in periodically inundated swamplands due to the changes of the water levels, may affect the release of metal (loid)s (e.g. As, Fe) into the groundwater (Karimian et al., 2017). The behavior and transport of As are closely related to the biogeochemical cycling of Fe, S and C (e.g. Bostick and Fendorf, 2003; O'Day et al., 2004; Root et al., 2009). Microbial sulfate (SO_4^{2-}) reduction, couples with the oxidation of organic matter (OM) or H_2, may also affect As behavior via the production of sulfide (S(-II)) (Barton, 1995, Poulton et al., 2004; Rochette et al., 2000, Muyzer and Stams, 2008). Under different conditions, HS^- can immobilize As by the precipitation of As sulfides (e.g. orpiment ($As_2S_{3(s)}$) and realgar ($AsS_{(s)}$)) if the As concentration is high enough (O'Day et al., 2004; Root et al., 2009), or form reduced inorganic sulfur such as $FeS_{2(s)}$ and $FeS_{m(s)}$ (Berner, 1970; Rickard, 2006; Rickard and Iii, 2007) onto which As can adsorb (Wolthers et al., 2005; R.M.M. Couture et al., 2013). Arsenic can also co-precipitate with iron sulfide minerals to form arsenic-substituted pyrite, known as "arsenian pyrite" (e.g. Rittle et al., 1995; Neuman et al., 1998; Charlet et al., 2011; Langner et al., 2012; Le Pape et al., 2017; Wang et al., 2018). Lastly, arsenite is known to bind strongly onto sulfhydryl groups (thiols) of OM (ThomasArrigo et al., 2016; Langner et al., 2013; R.M. Couture et al., 2013; Langner et al., 2012). The dominance of one mechanism over the other is determined by variety factors (e.g. aqueous As speciation, pH, Fe and S mineralogy) whose identification is complicated by dynamic conditions.

There is significant interest in elucidating the processes driving As mobility in sediments under sulfate reducing conditions and to understand hydrological transport controls on As fluxes from sulfate-rich sediments in the Mekong Delta (Métral et al., 2008; Buschmann and Berg, 2009). Nevertheless, experimental studies accurately isolating biogeochemical processes during the oscillating redox conditions in Vietnamese paddy fields and shallow aquifers are still scarce. In particular, the role of sulfate-reducing bacteria (SRB) and sulfate-oxidizing bacteria (SOB) in As immobilization in the sediment during redox dynamic conditions remain poorly defined at such sites. To determine the mechanisms controlling As mobility in sulfate-rich sediment of seasonally flooded soils, we investigated the As, Fe, and S species generated by oscillating redox conditions in laboratory experiments. We used automated bioreactors containing sediments with equal total As concentration and variable sulfate contents. A 16S rRNA amplicon analysis was performed to unravel the role of bacteria in the sediment through redox cycles and X-ray absorption near-edge spectroscopy (XANES) was exploited to reveal solid-phase As species.

2. Materials and methods

2.1. Field site characterization

2.1.1. The study area and sediment sampling

The seasonally flooded sediment was collected at the Quoc Thai commune, An Giang province, Vietnam, in a paddy soil near the Mekong River during the dry season, in 2014 (Fig. SI-1) where was contained a high As concentration in groundwater (Wang et al., 2018; Van Phan et al., 2017). A sediment core was drilled from a depth of 0–20 m and separated into sections as a function of depth under an argon (Ar) flux and then immediately placed in the heat sealed Mylar® bags under N_2 atmosphere (Wang et al., 2018). The sediment samples were shipped in a cooler with ice back to France and stored at +4 °C until processing. Peat-rich sediment from 16 m - deep layers was obtained for the batch experiments. All preparation and samples conditioning were performed in a Jacomex® under N_2 atmosphere ($O_2 < 10$ ppm) to ensure anoxic conditions.

2.1.2. Mineralogy and elemental composition analyses

The elemental composition was measured using the total acidic digestion (e.g. $HNO_3 + H_2O_2 + HF$, $H_3BO_3 + HF$) followed by Inductively Coupled Plasma – Optical Emission Spectrometry (ICP-OES) (Agilent 720-ES, Varian) (Cotten et al., 1995). X-ray diffraction (XRD) measurements were performed with CoKα radiation on a Panalytical® X'Pert Pro MPD diffractometer using a Debye–Scherrer configuration using an elliptical mirror to obtain a high flux and parallel incident beam, and an X'Celerator® detector to collect the diffracted beam. All sediment samples were transferred into glass capillaries inside a glovebox Jacomex® ($O_2 ≤ 10$ ppm) to avoid oxidation by air.

2.2. Experimental design and redox oscillation set-up

Two batch bioreactors, R1 and R2, were prepared with 1 L of sediment suspension containing 100 g of dry sediment (<1 mm fraction), arsenite (As(III)), and two different concentrations of sulfate (SO_4^{2-}). The contaminants were prepared by dissolving of sodium (meta)arsenite (NaAsO$_2$, ≥98%,Sigma-Aldrich) and sodium sulfate (Na$_2$SO$_4$(s), ≥99%, anhydrous, granular, Sigma-Aldrich), to obtain a solution with final concentration of 50 μM of As(III), 0.1 and 1 mM of SO_4^{2-} for R1 and R2, respectively. The suspensions were pre-equilibrated inside the glove box for 2 weeks before doing the redox experiments. More details of the reactor system were described in the previous studies (e.g. Parsons et al., 2013; Markelova et al., 2018; Phan et al., 2018). At the start of the redox experiment (t = 0), two mixture solutions containing the same concentration of As(III) and two different concentrations of SO_4^{2-} were added in the two reactors (R1 and R2). Cellobiose (C$_{12}$H$_{22}$O$_{11}$ – Sigma-Aldrich), a byproduct of microbial hydrolysis of cellulose (Lynd et al., 2002; Schellenberger et al., 2011), was manually replenished at the start of each anoxic half-cycles to obtain the final concentration of

DOC equal to 8.33 mM including the DOC in sediments. All input solutions were adjusted for ionic strength (I = 30 mM) using sodium chloride (NaCl - Sigma-Aldrich). Reactors were covered with aluminum foil to avoid the photo-degradation of organic matter and contaminants.

Reduced – oxidized oscillations were carried out by automatically modulating the influx gas between the mixture of N_2 and 300 ppm CO_2 in anoxic half-cycle (7 days) except for the first one with 5 days, and compressed air of 1% CO_2, 79% N_2 and 20% O_2 in oxic half-cycle (7 days) using an Agilent switching unit and a system of solenoid valves. Redox cycles were monitored for approximately 40 days. Gas flow rate and temperature were kept constant at 30 mL/min and 30 °C. Suspension samples were collected five days/week of each half-cycle for aqueous, solid phase and microbial analyses through a connection on the top of the reactors. Except for the days collecting the plus 5 mL slurry for microbial analysis, a 15 mL of suspension was collected in the other days. These suspensions were centrifuged at 14000 rpm for 20 min (Sigma 3-30 KS) to separate the solid phase (e.g. XRD and XANES analysis), while the supernatant was then filtered through cellulose hydrophilic 0.22 μm membrane (Chromafil RC, Roth). A part of supernatant was acidified with HNO_3 (2%, Sigma-Aldrich) or HCl (0.1 M, Roth) and preserved at 4 °C for total element concentration and DOC analysis, respectively. A 2 mL of supernatant was stored at 4 °C without acidification for anion measurement. The rest of supernatant, slurry samples were flash frozen using liquid nitrogen and kept at −80 °C for another aqueous and microbial analysis.

2.3. Aqueous phase characterization

All standards and reagents, were prepared with ultra-pure water, and were of analytical grade from Fluka, Sigma-Aldrich or Merck. The glass and plastic parts were firstly washed with 5% HNO_3 then with ultra-pure water (18 MΩ·cm^{-1}). The E_h and pH data were recorded automatically every 10 s using an Aligent 34970A BenchLink Data Logger through the E_h and pH electrodes (Mettler-Toledo Xerolyt Solid). Measured E_h value was corrected for the reference electrode's voltage (+207 mV) relative to the standard hydrogen electrode (SHE), and corresponded to the Ag/AgCl (3 M KCl) reference electrode. The pH electrodes were calibrated using the measured data of three-point using pH buffers of 4, 7 and 10 at 25 °C at the start and the end of experiment displaying that the electrode response were not shifted significantly. The real pH values were then calculated based on the calibration curves.

Analysis of total cations, including trace and major elements, were performed with ICP-OES (Agilent 720-ES, Varian) after dilution and acidification by ultrapure HNO_3 (2%, Sigma-Aldrich) with a detection limit of 0.02 and 0.1 mg·L^{-1}, respectively and a precision better than 5%. DOC was determined using a Shimazu VCSN analyzer (TOC-5000, Shimadzu) with a detection limit of 0.3 mg/L and a precision better than 2.5% for most samples. Nevertheless, it is important to note that for concentrations close to the detection limit, the precision can be significantly lower (50–100%). DOC tubes were heated at 400 °C for 3 h avoiding organic carbon contamination. Non-acidified samples were used to analyze major anions (e.g. F^-, Cl^-, NO_3^-, NO_2^-, Br^-, SO_4^{2-}, PO_4^{3-}) and acetate by ion chromatography using a Metrohm 761 compact ion chromatography with a detection limit of 0.1 mg·L^{-1} and a precision better than 5%. [Fe^{2+}] and [$S(-II)$] were determined photometrically on the sample filtered using the Ferrozine method (Lovley and Phillips, 1986; Viollier et al., 2000; Stookey, 1970) and Cline method (Cline, 1969), respectively. Standard stock solutions were prepared using $Na_2S * 9H_2O$ for the calibration curve of $S(-II)$ and $FeCl_2 * 4H_2O$ for the calibration curve of Fe^{2+}. The standards and samples were then measured immediately using UV–Vis spectroscopy (Lambda 35, Perkin Elmer) at 562 nm and 664 nm absorbance for Fe^{2+} and $S(-II)$, respectively.

Aqueous As species (e.g. As(III), As(V), MMA and DMA) were analyzed at Plateforme AETE – HydroScience/OSU OREME, Montpellier, France, using the coupling LC-ICP-MS system (Bohari et al., 2001). The detail condition was described in Phan et al. (2018). The detection limit was 0.09 μg/L for As(III), 0.06 μg/L for DMA, 0.04 μg/L MMA and 0.41 μg/L for As(V), with a precision better than 5%.

2.4. Microbial community analysis

The 16S rRNA gene diversity was accessed through paired-end Illumina MiSeq at Research and Testing Laboratory (Texas, USA) following the method of Zhang et al. (2014). Slurry samples were collected at the end of the reduced cycle and in the middle of the oxidized cycle in both reactors (Fig. 1a–b). The overall approach entails 16S rRNA gene amplicon sequencing as a function of time and geochemical conditions. A 0.25 g suspension sample was used for total geonomic DNA (gDNA) extraction using the PowerSoil® DNA Isolation kit (MO BIO Laboratories, Carlsbad, USA). The DNA quantification was determined using a Nanodrop 1000 Spectrophotometer (Thermo Fisher Scientific, USA). After the DNA quantification, the amplification of the 16S rRNA gene was followed by the polymerase chain reaction (PCRs) using the forward (28F, GAGTTTGATCNTGGCTCAG) and reverse (519R, GTNTTACNGCGGCKGCTG) primers that amplify the V1-V3 region (Fan et al., 2012) (Biometra T3 Thermocycler, Germany). The PCR reaction mix for amplification contained 5 μL 10 × PCR buffer, 1 μL dNTPs (10 mM), 2 μL each of the forward and reverse primer (5 μM) and 0.8 μL Taq polymerase and balance water with the total volume of 50 μL. The thermal program, set up of a 5 min at 95 °C, 1 min at 50 °C, 1 min at 68 °C, 34 cycles at 95 °C for 1 min/cycle, 10 min at 68 °C, was performed with the Lightcycler® 480 (Roche). PCR products were conceived on an agarose gel, and the 16S rRNA band excised and purified using the Wizard® SV Gel and PCR Clean-Up System (Promega, USA). The sequencing process of PCR 16S rRNA amplicons were merged, denosed, quality trimmed and demultiplexed using USEARCH (Edgar, 2013). These sequences were then clustered into operational taxanomic units (OTUs) using the UPARSE algorithm with a similarities higher than 97% (Edgar, 2013), and then checked for Chimera detection using UCHIME (Edgar et al., 2011). A summarized database of high quality sequences derived from the NCBI database was described in the OTUs table (Table 1), and the full data shown in Table S-3 (Supporting information).

2.5. Solid-phase characterization

2.5.1. X-ray absorption near edge structure (XANES)

Solid-phase samples were collected from the two reactors at the end of the redox cycles indicated in Fig. 1a–b. X-ray absorption near edge structure (XANES) was used to characterize both As and S speciation. S K-edge XANES data were collected at the XAFS beamline of the Elettra synchrotron (Trieste, Italy), whereas As K-edge XANES data were done at the bending magnet beamline BM08-LISA of the European Synchrotron Radiation Facility (ESRF, Grenoble, France).

Sulfur K-edge (2472 eV) measurements were performed using a Si (111) monochromator calibrated relative to the white line of a $Na_2S_2O_{3(s)}$ standard (Sigma-Aldrich) at 2471.64 eV. Spectra were collected in fluorescence mode using a solid-state Si detector. A commercial elemental sulfur reference was measured in fluorescence mode before each scan for accurate energy calibration. For the linear combination fitting (LCF) of XANES spectra at the S K-edge, the following suite of sulfur references was used: (i) FeS (mackinawite), synthesized under strict anoxic conditions with solutions obtained after dissolution of $FeCl_2 * 6H_2O$ and $Na_2S * 9H_2O$ salts, (ii) pure FeS_2 (pyrite) was synthesized according to the protocol described in Le Pape et al. (2017), (iii) S_8 (elemental sulfur, Sigma – Aldrich), and (iv) commercial K_2SO_4 (sulfate). Some of the reference compounds spectra (e.g. FeS, FeS_2 and K_2SO_4) were acquired on the 4–3 beamline at SSRL in the fluorescence mode.

For LCF of XANES spectra at the As K-edge, the following set of arsenic references compounds was considered: (i) $NaAsO_2$ and
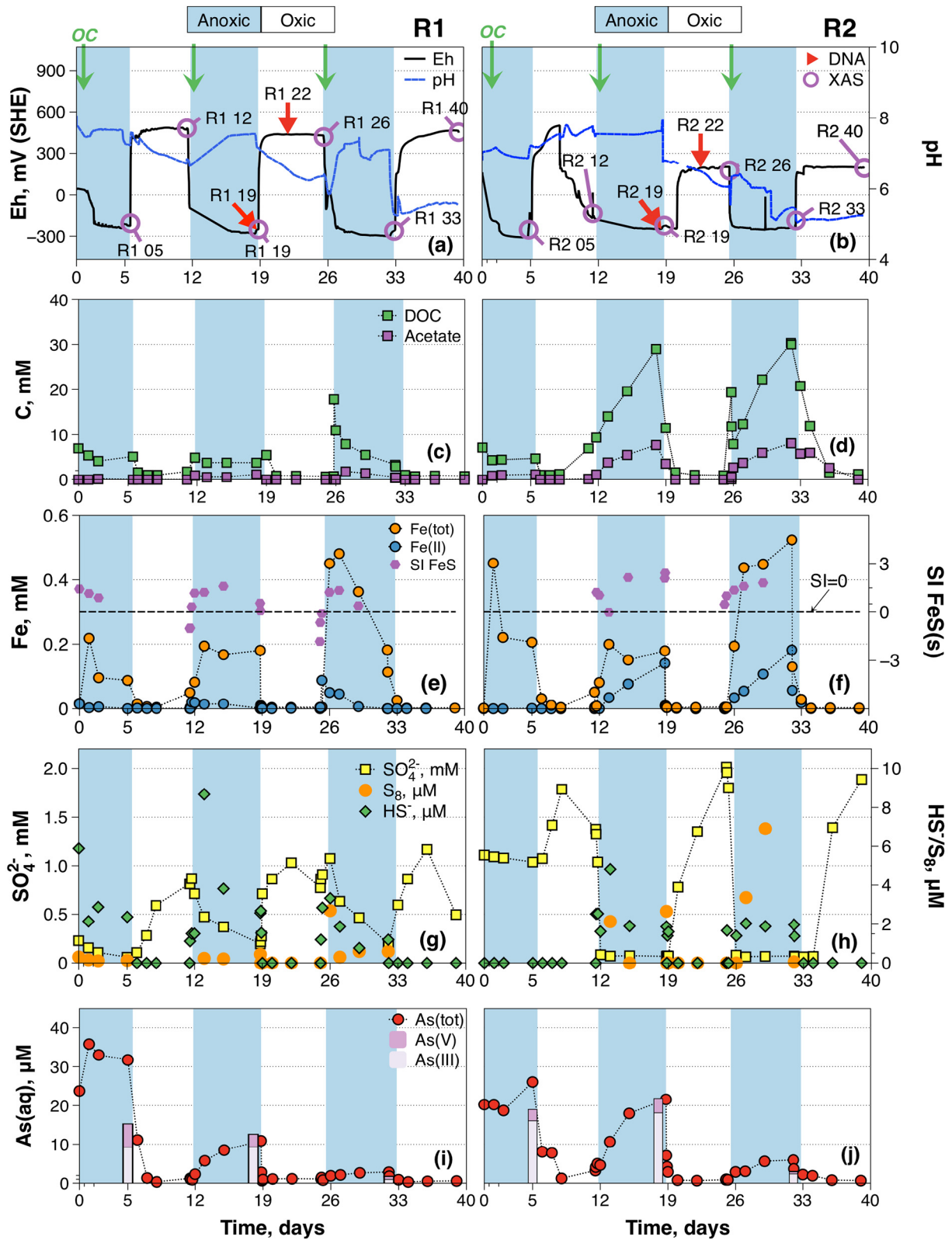
Fig. 1. Aqueous chemistry measured E_h (SHE) and pH (a–b), DOC and acetate (c–d), Fe(tot) and Fe^{2+} (e–f), S(tot) and SO_4^{2-}, HS^- and S_8 in suspension (g–h), As(tot), As(V) and As(III) (i–j) data with time in reactor R1 (0.1 mM SO_4^{2-}) (left) and R2 (1.0 mM SO_4^{2-}) (right). Blue and white shaded areas indicate the anoxic and oxic half-cycles, respectively. Sampling points for S K-edge XANES and microbial community analysis are shown on the E_h curve (As and S K-edge XANES = open purple circles, 16S rRNA = red arrows), cellobiose (OC) adding points = green arrows, and saturation index of porewaters (e–f) with respect to FeS. (For interpretation of the references to colour in this figure, the reader is referred to the web version of this article.)

NaHAsO$_4$ (Sigma-Aldrich), MTA(V) (monothioarsenate), DTA (V) (dithioarsenate), and TeTA(V) (tetrathioarsenate), prepared using the method of Schwedt and Rieckhoff (1996) and optimized by Suess

et al. (2009); (ii) As-bearing minerals from natural deposits were considered such as orpiment (As$_2$S$_3$), realgar (AsS), arsenian pyrite (As-substituted FeS$_2$), and arsenopyrite (FeAsS) (Le Pape et al., 2017), (iii)

Table 1
Analysis of taxa (contribute ≥1% of OTUs) corresponding to potential metabolism and oxygen tolerance of selected samples at R1 and R2.

Species	% OTUs				Potential metabolism	O2 tolerance	References
	R1–19 Anoxic	R2–19 Anoxic	R1–22 Oxic	R2–22 Oxic			
Arcobacter sp.	60.487	2.931	0.862	1.077	Sulfide oxidizing	Microaerophilic, autotrophic	Wirsen et al., 2002
Klebsiella sp.	6.381	10.511	3.704	2.735	Fermentation	Microaerophilic–aerobic	Franciscon et al., 2009
Rhizobium sp.	2.804	3.328	2.725	1.668	Nitrogen fixing	Microaerophilic	Schmeisser et al., 2009
Geobacter bremensis	2.490	5.109	2.690	5.674	Iron and sulfur reduction	Aerotolerant	Snoeyenbos-West et al., 2000
Clostridium sp.	2.158	2.435	3.253	3.295	Iron and sulfur reduction	Microaerophilic	Dobbin et al., 1999; Li et al., 2011; Thabet et al., 2004
Acidovorax delafieldii	2.147	0.405	1.735	0.507	Definication	Aerobic	Willems and Gillis, 2015
Hydrogenophaga taeniospiralis	2.020	3.095	7.484	5.679	Hydrogen oxidizing	Microaerophilic–aerobic	Willems et al., 1989
Acinetobacter sp.	1.879	0.124	2.637	0.847	Methane oxidation	Aerobic	Wang et al., 2012
Hydrogenophaga pseudoflava	1.624	8.728	1.582	1.255	Hydrogen oxidation, thiosulfate oxidation	Microaerophilic–aerobic	Willems et al., 1989; Graff and Stubner, 2003
Thiobacillus thioparus	0.466	2.388	0.211	0.251	Iron and sulfide oxidation	Microaerophilic–aerobic	Hedrich et al., 2011b
Candidatus accumulibacter sp.	0.788	1.690	4.689	2.986	Iron oxidizing	Microaerophilic–aerobic	Hedrich et al., 2011a
Geobacter sp.	0.237	1.628	3.311	19.114	Iron and sulfur reduction	Microaerophilic	Snoeyenbos-West et al., 2000, Lin et al., 2004
Rhodobacter sp.	0.095	1.447	1.371	3.263	Iron oxidation	Microaerophilic–aerobic	Poulain and Newman, 2009
Thiobacillus sp.	0.120	1.083	0.064	0.178	Iron and sulfide oxidation	Microaerophilic–aerobic	Poulain and Newman, 2009
Gemmobacter sp.	0.343	1.076	0.955	0.847	Carbon and nitrogen degradation	Facultative anaerobic	Kumaresan et al., 2015
Flavobacterium sp.	0.011	1.026	0.000	0.000	Decompose several polysaccharides	Aerobic	Schellenberger et al., 2011
Rhodobacter capsulatus	0.198	0.745	15.619	10.987	Fe(II) oxidation	Microaerophilic–aerobic	Hedrich et al., 2011b
Dechloromonas hortensis	0.304	0.793	2.837	1.072	Organic matter degradation	Aerobic	Wolterink et al., 2005
Vogesella indigofera	0.035	0.064	1.993	1.229	Organic matter degradation	Aerobic	Luan & Medzhitov, 2016
Sulfurospirillum sp.	0.735	0.050	1.178	1.914	Sulfur reduction	Microaerophilic	Tang et al., 2009
Desulfobulbus sp.	0.286	0.600	0.615	1.537	Sulfate reducing	Anaerobic	Muyzer and Stams, 2008; Pokorna & Zabranska, 2015
Desulfomicrobium sp.	0.102	0.231	0.820	1.517	Sulfate reducing	Anaerobic	Muyzer and Stams, 2008; Pokorna & Zabranska, 2015
Prolixibacter sp.	0.512	0.969	0.399	1.412	Fermentation	Microaerophilic	Holmes et al., 2007
Novosphingobium sp.	0.441	0.857	0.586	1.124	Organic matter degradation	Microaerophilic	Nguyen et al., 2014

As(III)- and As(V)-sorbed ferrihydrite were used as proxies for As(III)-O and As(V)-O local molecular environments (Hohmann et al., 2011; Ona-Nguema et al., 2005) and (iv) glutamyl-cysteinyl-glycinyl-thiolarsenite (As(III)-Glu) synthesized using the method of Miot et al. (2008) was used as representative of thiol bound As(III) organic matter (OM) species (see in Table S-4 in Supporting information for more details on the references used). Some of the reference compounds spectra (e.g. arsenian pyrite and thiol-bound As(III)) were collected at 15 K in fluorescence mode at the SAMBA beamline at SOLEIL synchrotron (Phan et al., 2018).

Both of As and S XANES data analysis were performed using the Athena software (Ravel and Newville, 2005) and the relative contributions of the different compounds to the sample spectra were achieved by linear combination fitting (LCF). A homemade program based on a Lenvenberg-Marquardt algorithm was used to improve the fit quality following the method of Resongles et al. (2016), which was described in detail in Phan et al. (2018).

2.5.2. Acid-volatile sulfide and elemental sulfur analysis

To complement the S K-edge XANES results, we measured acid-volatile sulfide (AVS) (Hsieh et al., 2002; Burton et al., 2008; Couture et al., 2016). AVS extraction was based on a purge and trap method (Allen et al., 1993), which relies on the conversion of sulfur compounds within sediments after centrifuging and keep dry in the glovebox that are first purged with HCl to generate volatile H_2S, and secondly trapped with NaOH. Finally, a complexation is done by adding a diamine reagent to the trapped solution to form a methylene blue molecule (Cline, 1969), which is quantified by UV spectroscopy at 670 nm. The calibration curve was performed by the same method using Na_2S solution at 10 mM. AVS purge and trap measurements were carried out within airtight Teflon reactors

under continuous flow of nitrogen to avoid oxidation of sulfide. A quantity of 0.18 to 0.50 g of previously freeze-dried sediment was used for AVS extractions and quantification.

The amount of sulfur that remained in the solid phase at the surface in the form of elemental sulfur (S_8) was analyzed using a perchloroethylene extraction combined with High Performance Liquid Chromatography (HPLC) following the method described in McGuire and Hamers (2000). Perchloroethylene-extractable sulfur was obtained after pretreatment of unfiltered samples with 250 μL of ZnAc (5%) to precipitate free sulfide (Wan et al., 2014). Sulfide fixation allows ZnAc to react with S(-II) as well as with S_n^{2-} (n ≥ 2, polysulfides) leading to the precipitation of ZnS. After 10 min, 4 mL of perchloroethylene was injected into 0.5 mL of suspensions. The samples were shaken for 3 h and filtered through 0.22 μm pore size membranes. The supernatants were then analyzed by HPCL (PerkinElmer 2000 pump and auto-sampler, UV–vision detectors and software AZUR V6.0 software) using a C18 column (Nucleosil 100-5PAH) and isocratic elution in methanol 95% at a flow rate of 0.4 mL/min. The detection was performed at a wavelength of 265 nm.

2.5.3. Quantitative total As concentration

To determine the bulk As concentration, sediment samples, collecting in the end of each anoxic an oxic half-cycles, were dissolved completely using a hot plate digestion (Cotten et al., 1995). About 50 mg of dried and homogenized sample were first added with 0.84 mL of distilled HNO_3 (14 N) and 0.2 mL of H_2O_2 to dissolve organic matter, then followed by mixing of 0.4 mL of distilled HF (48%) under a fume hood, and put on a hot plate at 80 °C for 3 days. This solution was let cool down before adding 20 mL of H_3BO_3 (4.5%). The final extract was diluted with MilliQ water to 250 mL and analyzed for total As concentration using ICP-AES.

2.6. Thermodynamic modeling

Thermodynamic calculations were performed using the PHREEQC program version 3.3.10 (Parkhurst and Appelo, 2013). The following calculations were performed: (i) thermodynamic aqueous species distribution during the anoxic and oxic half cycles, and (ii) the saturation indices ($SI = \log IAP/K_{sp}$) at each sampling point with respect to solid arsenic, sulfur and iron phases. The WATEQ4F database for the As species was updated according to the data reported in the literature (Helz and Tossell, 2008). The added species included As(III) species ($H_nAsO_3^{n-3}$) (As(III) – arsenite), $H_nAsO_4^{n-3}$, $H_nAsSO_2^{n-3}$ (MTA(III) – monothioarsenite), $H_nAsS_2O^{n-3}$ (DMAs(III) – dithioarsenite), H_nAsS_3 (TTA(III) – trithioarsenite), and As(V) species ($H_nAsO_4^{n-3}$ (As(V) – arsenate), $H_nAsSO_3^{n-3}$ (MTA(V) – monothioarsenate), $H_nAsS_2O_2^{n-3}$ (DTAs (V) – dithioarsenate), $H_nAsS_3O^{n-3}$ (TTA(V) – trithioarsenate) and $H_nAsS_4^{n-3}$ (TeTA(V) – tetrathioarsenate)). Their reactions and equilibrium constants are summarized in Table S-1 in Supporting information.

3. Results

3.1. Aqueous chemistry

The aqueous phase results of the redox experiments carried out in reactors R1 and R2, containing respectively with 0.1 mM and 1 mM of sulfate, are summarized in Fig. 1.

3.1.1. E_h and pH cycling

The reducing and oxidizing steps can be clearly identified monitoring the E_h and pH values as a function of time (Fig. 1a–b). E_h ranges from −300 mV, in anoxic half-cycles, to +500 mV, in oxic half-cycles, and pH varied in the range between 5.2 and 7.8 for both reactors. E_h and pH underwent repeated cycling in the low sulfate reactor (R1). However, in the high sulfate reactor (R2), oxidizing conditions were not fully attained in all cycles. Reducing half cycles were characterized by a decrease in E_h and an increase in both pH and in the Fe^{2+} concentration, while the oxidizing half cycles showed opposite trends (Fig. 1a–b). Intra-cycle E_h changes were similar to the E_h-monitoring studies of flooded soils and previous redox oscillation experiments (Couture et al., 2015; Parsons et al., 2013; Thompson et al., 2006). In the reductive processes, the decrease in E_h may be driven by the consumption of successive terminal electron acceptors, such as Fe(III) and SO_4^{2-} coupled to DOC oxidation by the microbial community (Essington, 2004), which resulted in hydroxyl (OH^-) production and pH increase.

3.1.2. DOC cycling

A 8.33 mM of DOC was manually replenished after adding cellobiose at the start every anoxic half-cycle (Fig. 1c–d). During the oxic half-cycle, in both reactors, DOC decreased significantly together with the low concentration of acetate during each oxic half-cycles probably due to respiration oxidation of Fe^{2-}, S(-II) and As(III). During the anoxic half-cycle, in R1 DOC also decreased slightly, while in R2 with higher SO_4^{2-}, DOC increased significantly together with an increase production of acetate. This is probably due to the release of DOC from sediment was greater in amount of DOC consumption by heterotrophic bacteria (Parsons et al., 2013).

3.1.3. Total Fe and Fe(II) cycling

In both reactors, [Fe] and [Fe^{2+}] increased in the reducing cycles, consistently with the reduction reaction of labile Fe-oxides (Essington, 2004; Thompson et al., 2006). During the oxic cycles, [Fe^{2+}] dropped when E_h values increased indicating that Fe^{2+} originating from initial pyrite oxidation and Fe-(oxyhydr)oxides was oxidized to Fe(III), which precipitated as poorly soluble phases, e.g. ferrihydrite and goethite. Furthermore, thermodynamic predictions suggest that in anoxic sulfidic conditions, mackinawite ($FeS_{(s)}$) is the first iron sulfide to precipitate, and it constitutes a major component of the empirically defined "acid volatile sulfides" (AVS) (Rickard and Morse, 2005). The saturation index of FeS (SI > 0) was calculated using PHREEQC in both reactors and is reported in Fig. 1e–f.

3.1.4. S cycling

[SO_4^{2-}] decreased during the anoxic half-cycles and increased during the oxic half-cycles and reached about 1.1 mM in R1 and 2 mM in R2, respectively, both were >1 mM, compared to the added SO_4^{2-} of 0.1 mM at R1 and 1 mM at R2. This difference is probably due to the oxidation of pyrite from the sediment (Fig. 1g–h). Additionally, complete [S(-II)] depletion was observed during the oxidation cycles, while in reduction cycles, [S(-II)] varied in the range between 0.8–8.7 μM in R1, and 1.4–4.8 μM in R2 (Fig. 1g–h). Low [S^0] was detected in supernatants, which is consistent with the fact that elemental sulfur is typically associated with the solid phase (S_8) (McGuire and Hamers, 2000; Wan et al., 2014). [S_8] was found in the suspension at concentration ranges between 0.06–8.7 μM and 0.1–2.7 μM in R1 and R2, respectively. This finding suggests that sulfate reduction were followed by sulfide oxidation to sulfur and sulfate.

3.1.5. As cycling

Intra-cycle mobilization of aqueous As was observed during the anoxic half cycles. Particularly, As was released in the initial anoxic half-cycle, reaching up to 32 μM and 27 μM in R1 and R2, respectively, and then sequestered in the solid phase in subsequent anoxic cycles. Conversely, oxidizing conditions re-immobilized As, returning to a base-level of approximately 1 μM in both R1 and R2. The As decreasing trend and the concomitant increasing in E_h were observed (Fig. 1k–l). When the oxidizing condition prevail, the most thermodynamically favorable As species was As(V) ($H_2AsO_4^-$ and $HAsO_4^{2-}$). The reducing condition was established during the anoxic half-cycles, which favors the formation of arsenite (H_3AsO_3). Successive redox cycles resulted in 92% and 83% removal of total dissolved As in R1 and R2, respectively.

3.2. Microbial community analysis

Operational taxonomic unit (OTU) libraries were generated for the samples from day 19 (anoxic, R1- or R2–19) and 22 (oxic, R1- and R2–22), as shown by the red arrows in the Fig. 1a–b. Numerous bacterial phyla were identified in the microbial community during the reducing and oxidizing phases mainly consist of Proteobacteria including Alpha-, Beta-, Gamma-, Delta- and Epsilon-proteobacteria classes, and the phyla Bacteroidetes and Firmicutes. The full data are presented in Table S-3, Supporting information.

In reactor R1, there were only three phylotypes that we more abundant under anoxic condtions than under oxic conditions and present at >1% of OTUs: *Arcobacter* sp., represented the largest group in R1, with >60% of the OTUs, *Klebsiella* p., representing ~6% of the OTUs, and *Acidovorax* sp., representing 2% of the OTUs in R1. The first two organisms were also more abundant under anoxic conditions in R2 (Table 1).

In contrast, and somewhat surprisingly, taxa related to SRB and iron-reducing bacteria were detected under both oxic and anoxic conditions. *Geobacter* species (*Geobacter* sp. and *Geobacter bremensis*), known iron and sulfur reducers, were enriched in the two experiments (R1 and R2) during both the oxic and anoxic cycles, representing ~2.7 and ~6.7% (anoxic and oxic, respectively) of the OTUs in R1 and ~6 and ~25% of the OTUs in R2 (anoxic and oxic, respectively). SRB, including *Desulfobulbus* sp., *Desulfomicrobium* sp., and *Desulfovibrio* sp., were detected in both reactors with higher contributions in reactor R2 than in reactor R1 (Table 1).

In the oxic half-cycles, taxa including iron- and sulfur-oxidizing bacteria such as *Thiobacillus* sp. were detected suggesting the

microbial oxidation of Fe^{2+}, S^{2-} or sulfur (Hedrich et al., 2011b). This was particularly true for R1 (*Thiobacillus* sp. represented 3.3% of OTUs) and less so for R2 (0.4% of OTUs). Iron oxidizers, e.g. *Rhodobacter* sp., potentially able to use reduced sulfur compounds (S^0, HS^-, $S_2O_3^{2-}$), H_2, or organic compounds as electron donors, were also identified, particularly in R2 (17% and 14.3% of OTUs in the anoxic and oxic half-cycle, respectively). Additionally, the genus *Hydrogenophaga* sp., are facultatively autotrophic aerobic hydrogen-oxidizing bacteria (Willems et al., 1989) and OTUs related to this genus were predominantly identified in the oxic phase in R1 (11.8% of OTUs in oxic and 3.6% in anoxic) and in the anoxic phase in R2 (7.2% of OTUs in oxic and 9.3% in anoxic).

Finally, the presence of many heterotrophic bacteria, capable of operating under both aerobic and anaerobic conditions, such as *Rhizobium* sp. and *Klebsiella* sp., may account for the oxidation of OM during both phases (Eller and Frenzel, 2001; Francisco et al., 2009). Other heterotrophic bacteria, OM respiring bacteria, take a prominent part of the overall community in both reactors representing from 17 to 45% of total OTUs (Table 1).

3.3. Solid sulfur and arsenic dynamics

The initial anoxic sediments contained 32.1 g/kg dry sediment organic C, 0.7 g/kg total S, 15.6 g/kg total Fe (Table S-1). Smectite, quartz, muscovite, chlorite, albite, and pyrite were identified in the input sediment (Table S-1). The total As content was lower than detection limit as determined by total digestion and ICP-MS, but As K-edge XANES indicated that As was initially present in the O-bound As(V) and As(III) oxidation states, S bound As(III), and arsenian pyrite.

3.3.1. Solid S speciation

LCF of the XANES spectra at the S K-edge revealed that the majority of S accumulated in R1 and R2 as $FeS_{2(s)}$, sulfate (SO_4) and S_8, (Fig. 2 and Table 2). Most S was in the form of $FeS_{2(s)}$ during the last anoxic cycles (e.g. samples R1 33, R2 33). While S_8 mostly deposited in R1 during the anoxic half-cycles, about 11% of S_8 rested in the second oxic half-cycle, and increased to 22% in the last anoxic half-cycle (Table 2). The AVS values indicated of 1.8 and 0.17 $\mu M \cdot g^{-1}$ dry sediment during the second anoxic cycles (e.g. samples R1 19, R2 19), respectively (Table 2), while S spectra show that the fitting procedure with $FeS_{(s)}$ was not obtained a good result.

3.3.2. Solid As speciation

To determine the effect of redox cycling on solid arsenic speciation, X-ray absorption spectra were recorded at the As K-edge and the bulk As concentration was analyzed using total digestion on sediments sampled at the end of each half-cycle for both reactors, and on the initial sediment. It is worth noting that linear combination fitting XANES analysis is able to detect only species that are present in amounts higher than 5–10%, and to distinguish only species with sufficiently different spectral features. Arsenic K-edge XANES data suggested the presence of four distinct As species (Figs. 3, 4). The initial sediment included O-bound As(V), O-bound As(III), S-bound As(III), and arsenian pyrite (i.e arsenic-substituted pyrite) (Fig. 3). The bulk As concentrations in the same samples were analyzed using total digestion and ICP. The total concentration of As during the oxic conditions were higher than during the anoxic conditions in both reactors (Fig. 4). An increasing As trend in the sediment during the anoxic half-cycles were also observed. The presence of an admixture of O-bound As(III) and O-bound As(V) species in all samples, with an increase in the proportion of As(V) over As(III) during the oxidizing cycles (Fig. 4). In the last oxic cycle, the difference between As(V) and As(III) is quite small: 57% (or 53%) of As(V) and 44% (or 47%) of As(III) (Table 3, Fig. 4). In R1, in the anoxic half cycles, and partly also in oxic half cycles, 8–15% of the total As solid phase was attributed to thiol-bound As(III) (Figs. 3, 4a). In R2,
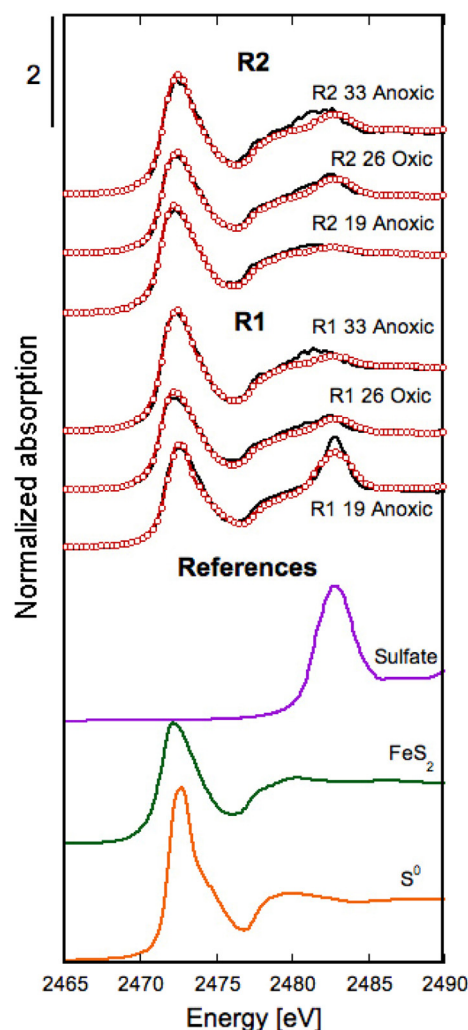
Fig. 2. Normalized S K-edge XANES spectra of sediment samples collected from reactors R1 (0.1 mM SO_4^{2-}) and R2 (1 mM SO_4^{2-}) at the end of each anoxic or oxic half-cycles, as shown in Fig. 1. The spectra of the samples (open circles) are reported together with the LCF curves superimposed (solid lines). The spectra of the reference compounds used for LCF (K_2SO_4, S_8 and FeS_2) are also shown. All spectra are vertically shifted for clarity.

LCF suggested that S-bound As compounds contributed to 8–16% of the total As, but they were not found to contribute in the last cycles, both R1 and R2 (Figs. 3, 4b).

Table 2
Solid-phase sulfur speciation. Proportion of the different S solid phases in the sediment samples by applying a linear combination fitting (LCF) procedure on XANES spectra at the S K-edge (Fig. 2). The error on percentages is estimated to be in the range between 5 and 15%. The acid volatile sulfide (AVS, $\mu mol/g$ of dry soil) was calculated from sequential extractions. Goodness of fits is estimated by the reduced chi-square ($Red\chi^2$) values.

Sample	AVS ($\mu mol/g$)	LCF (%)			$Red\text{-}\chi^2$ ($\times 10^2$)
		K_2SO_4	S_8	FeS_2	
R1 19	1.817	35	38	27	3.9
R1 26	–	15	–	85	1.8
R1 33	–	10	13	77	2.7
R2 19	0.167	8	–	92	1.2
R2 26	–	19	11	70	1.5
R2 33	–	16	22	63	3.9

◻ Anoxic (shaded)
◻ Oxic
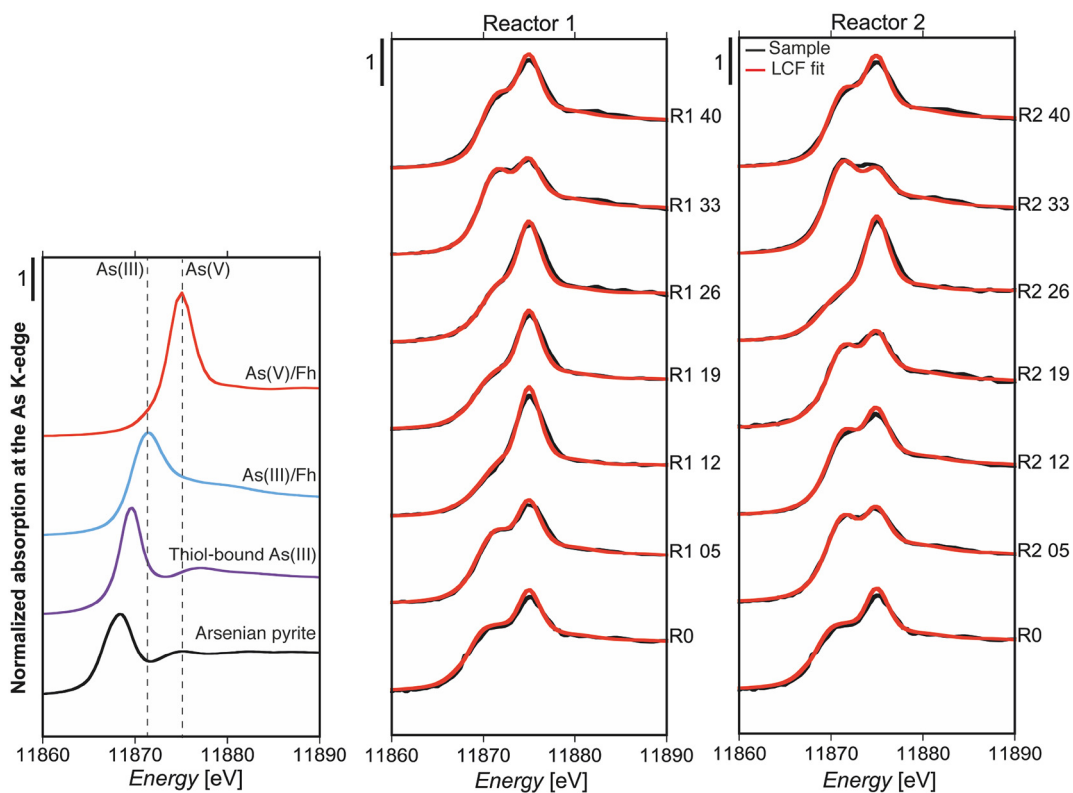
Fig. 3. The spectra of the reference compounds used for LCF (As(III/V) goethite, FeAsS, As$_2$S$_3$, thiol-bound As(III) are shown. Normalized As K-edge XANES spectra of sediment samples collected from reactors R1 (0.1 mM SO$_4^{2-}$) and R2 (1 mM SO$_4^{2-}$) at the end of each anoxic or oxic half-cycle, as shown in Fig. 1. The spectra of the samples (open circles) are reported together with the LCF curves superimposed (solid lines). All spectra are vertically shifted for clarity.

4. Discussion

4.1. Microbial sulfate reduction and sulfide oxidation

The analytical results of pore water and microbial analysis in both reactors suggest the occurrence of Fe and SO$_4^{2-}$ reduction during the anoxic half-cycles. Sulfate-reducing microorganisms (e.g. *Desulfobulbus* sp., *Desulfomicrobium* sp. and *Desulfovibrio* sp.) and iron-reducing ones (e.g. *Geobacter* sp., *Dechloromonas* sp.) were detected, supporting the occurrence of microbial SO$_4^{2-}$ and Fe reduction processes are ongoing. The detected species claimed to be involved in arsenate-respiration in the mobilization of As in Mekong Delta region (Héry et al., 2008, 2015; Lear et al., 2007; Rizoulis et al., 2014). It was surprising that *Geobacter* species were more abundant during oxic half-cycles than anoxic half-cycles. *Geobacter* species were previously considered strict

anaerobes (Caccavo et al., 1994; Lin et al., 2004). However, evidence of the use of oxygen as a terminal electron acceptor by some *Geobacter* species have emerged as has their ability to reduce O$_2$ under microaerophilic conditions (Lin et al., 2004; Parsons et al., 2013). Sulfate-reducing bacteria (SRB), such as *Desulfovibrio* sp., were also observed in oxic half-cycles. *Geobacter* species, can survive oxygen exposure and also contain enzymes to reduce oxygen (Cypionka, 2001). Nonetheless, these findings suggest the persistence of anaerobic micro-environments in which these organisms are able to grow during the nominally oxic phase. It can be hypothesized that the duration of the half-cycles was sufficient to lead to bulk geochemical parameters, indicating oxic conditions but probably not to fully oxidize microenvironments in the reactor.

Typically, carbon compounds are incompletely oxidized to acetate by SRB, which may explain the accumulation of acetate under anoxic
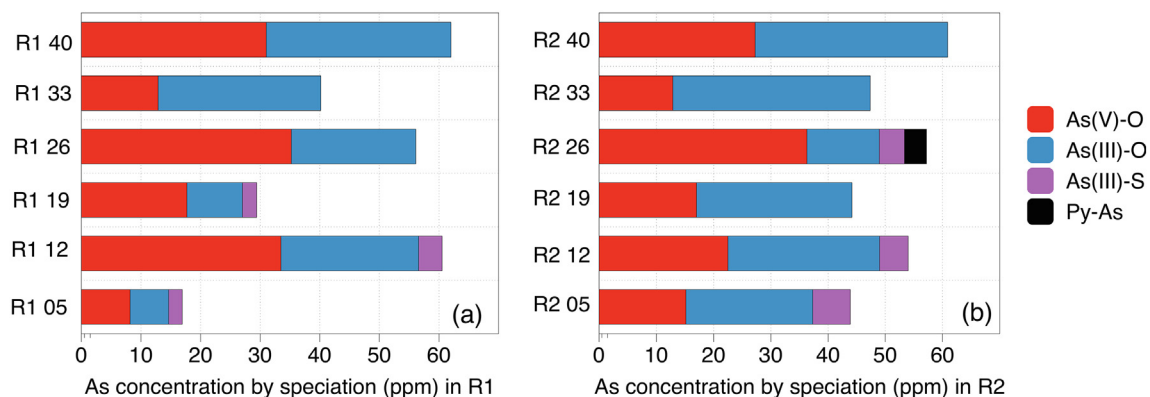
Fig. 4. Arsenic quantitative speciation in reactors (a) R1 (0.1 mM SO$_4^{2-}$) and (b) R2 (1 mM SO$_4^{2}$) at the end of each anoxic or oxic half-cycles. The As speciation is estimated by multiplying total As concentration sediments samples analyzed using the total digestion (the fraction of As as each of four species was obtained by LCF of As K-edge XANES data).

Table 3
Solid phase Arsenic speciation. Proportion of the different As solid phases in the initial sediment sample (R0) and in sediments extracted from bioreactors (R1 and R2) as revealed by applying a linear combination fitting (LCF) performed on the corresponding XANES spectra. The error on percentages is estimated to be in the range between 5 and 10%. Goodness of fits can be estimated by the reduced chi-square (Redχ^2) values.

Sample	LCF (%)				Red-χ^2 ($\times 10^3$)
	As(V)-O	As(III)-O	As(III)-S	Py-As	
R0	40	34	15	14	1.5
R1 05	43	47	12	–	1.0
R1 12	68	27	8	–	1.8
R1 19	59	31	8	6	1.1
R1 26	64	38	–	–	1.9
R1 33	33	70	–	–	0.7
R1 40	50	53	–	–	1.1
R2 05	37	54	16	–	0.7
R2 12	45	53	10	–	1.0
R2 19	37	59	–	–	0.9
R2 26	66	23	8	7	0.5
R2 33	28	75	–	–	0.7
R2 40	47	58	–	–	0.8

▨ Anoxic
☐ Oxic

conditions in R2 and, to lesser extent in R1. Coincidentally, Fe(II) and S(-II) were released repeatedly during three anoxic half-cycles for both high and low sulfate contents. These results seem to indicate an increasing trend in iron and sulfate reduction activities with the increase in sulfate concentration.

Arcobacter sp. represents 60% of the OTUs in the anoxic half-cycle in R1. There are several possible interpretations for the predominance of this genus. One is that the *Arcobacter* species is a microaerophilic sulfide oxidizer and has grown in the reactor during the anoxic phase, as dissolved oxygen concentrations were decreasing. The time point at day 19, simply might represent the anoxic end point of prolonged microaerobic conditions. Another explanation may be that this particular species is capable of reducing sulfur or other intermediate valence sulfur compounds. The prevalence of *Hydrogenophaga* sp., which are typically aerobic hydrogen oxidizers, during the anoxic half-cycle of R1 reactor would support the first interpretation.

Typical aerobic sulfide oxidizing bacteria, such as *Thiobacillus* sp. *Rhodobacter* sp., were also relatively abundant in oxic cycles, particularly in R2. These organisms are typically phototrophic, anaerobic iron oxidizers. However, since the reactors were wrapped in aluminum foil, phototrophy seems unlikely. They are also chemotrophs and it is conceivable that they could oxidize sulfide anaerobically with nitrate as an electron acceptor (Cytryn et al., 2005).

4.2. Mechanism of As mobility during redox oscillation

4.2.1. Control on As release under oxic condition

During the oxic half-cycles, 92% and 83% of dissolved As was removed in R1 and R2, respectively. Moreover, As K-edge XANES spectra show that O-bound As(V) and As(III), which can sorb onto Fe-(oxyhydr)oxides were the main As solid phase species in R1 and R2 (Fig. 4; Table 2). Other forms of As species, present in the initial sediment (e.g. arsenian pyrite and thiol bound As(III)), were absent in the oxic half-cycles, probably due to their oxidation. The ratio of As(V)/As (III) increased in the first two oxic half-cycles, and remained constant in the last oxic half-cycle. The precipitation of arsenic pentoxide (As_2O_5) may occur during the oxidation process. Although, calculations performed at pH values of 5.5–5.7 (SI of arsenic pentoxide (As_2O_5) ≥ 4.5), indicated that As_2O_5 may form in both R1 and R2 during the

oxic half-cycles, As_2O_5 is not detected due to a problem of nucleation. Adsorption onto freshly formed Fe-(oxyhydr)oxides is the most likely mechanism to explain its removal from the aqueous phase in nature or through the redox cycling batch experiments (Nickson et al., 2000; van Geen et al., 2003; Root et al., 2007; Couture et al., 2015; Parsons et al., 2013). Altogether, these results suggest that As immobilization during the oxidizing conditions is controlled by As adsorption on Fe-(oxyhydr)oxides.

4.2.2. Control on As release under anoxic condition

Under anaerobic conditions, microbially driven oxidation of organic matter coupled to the dissimilatory reductive dissolution of As-bearing Fe-(oxyhydr)oxides is commonly accepted to cause the transfer of As from the solid to the aqueous phase (Anawar et al., 2003; Hoque et al., 2009; Horneman et al., 2004; Nickson et al., 2000). As observed in a previous study performed on the same core of sediment collected in An Giang (Vietnam), under the effect of pyrite oxidation, which inhibits the sulfate-reducing bacteria, dissolved As was backfilled cycle after cycle (Phan et al., 2018). In contrast, this study shows that the successive anoxic half-cycles exhibit a decreased concentration of dissolved As (e.g. 92% in R1 and 83% in R2), and that As does not desorb at the end of the experiment, at both different sulfate concentrations (Fig. 1). This demonstrates that microbial SO_4^{2-} reduction led to the sequestration of a portion of aqueous As.

The formation of As sulfide precipitations (e.g. orpiment ($As_2S_{3(s)}$) and realgar ($AsS_{(s)}$)) is one of the possible mechanisms to remove As from the aqueous phase by direct reaction with dissolved S(-II) (R.M. Couture et al., 2013; O'Day et al., 2004). In this study, thermodynamic calculations indicate that $AsS_{(s)}$, $As_2S_{3(s)}$, and amorphous As sulfide ($As_2S_{3(s)}$) were slightly oversaturated by SI of 0.7, where HS^- is estimated at the maximum aqueous sulfide concentration (e.g. 8 and 5 µM in R1 and R2, respectively), and at slightly acidic to quasi-neutral pH (Fig. 5). In contrast, As K-edge data suggest no evidence for the formation of $AsS_{(s)}$ and $As_2S_{3(s)}$ during each 7-day anoxic half-cycles. This is probably due to low sulfide concentration and slow kinetics (Burton et al., 2013).

Another mechanism is linked to thiols formed during OM sulfurization (R.M. Couture et al., 2013). Recently, Wang et al. (2018) have reported the accumulation of thiol-bound As(III) in an organic-rich sediment of the Mekong Delta in Vietnam. Our finding of S-bound As(III) species in the initial samples are consistent with this. However, over successive redox cycles, As K-edge XANES data suggest that S-bound As(III) gradually decreased and remained negligible in the last anoxic half-cycle in both reactor (Fig. 4). Since the high porewater Fe (II) concentration favorably buffers aqueous S(-II) to very low concentration, it subsequently limits the sulfurization of organic matter (Burton et al., 2014). Consequently, in the successive cycles, the thiol bound As(III) complex formation is unlikely to be a dominant mechanism of aqueous As immobilization.

Arsenic may also sorb onto mackinawite ($FeS_{(s)}$) under the effect of microbial SO_4^{2-} reduction (Burton et al., 2014). The thermodynamic calculation also indicates that $FeS_{(s)}$ was oversaturated during anoxic half-cycles (Fig. 1e–f). However, the S K-edge XANES data indicated the presence of S(-II) and S^0, which suggests that the experimental conditions might be favorable for pyrite formation rather than FeS precipitation (Berner, 1970; Raiswell and Berner, 1985; Hurtgen et al., 1999). In agreement, As K-edge results showed no evidence for As(V) or As(III) adsorption onto Fe sulfides during redox cycling experiments. Hence, the As sequestration on $FeS_{(s)}$ may be marginal.

The actual As-sequestration mechanism could be the sorption of As on $FeS_{2(s)}$, a dominant Fe sulfide detected by S K-edge XANES investigation. The As(III) and As(V) species often sorb more strongly than the thioarsenates onto Fe-(oxyhydr)oxides and $FeS_{(s)}$, whereas MTA (V) sorbs most strongly on FeS_2 and leads to O-bound As(III), because thiorarsenics donate S atoms to FeS_2 (R.M.M. Couture et al., 2013). Based on the thermodynamic modeling constants, As species are
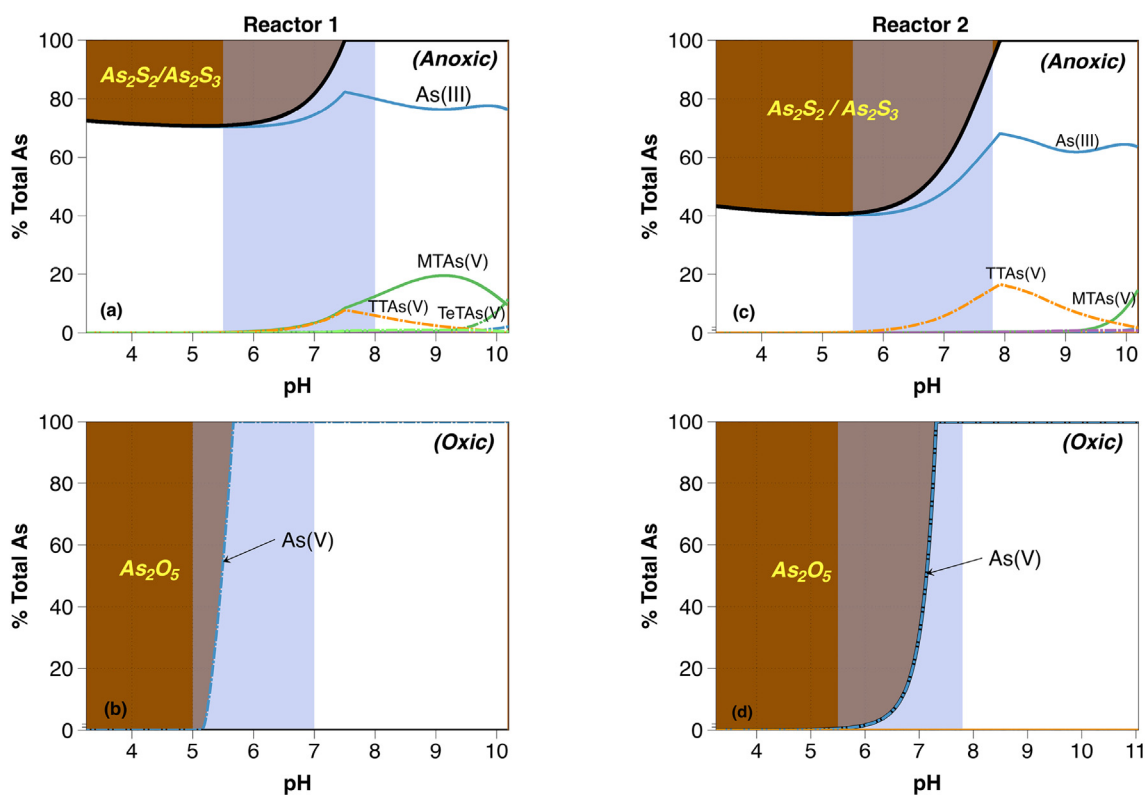
Fig. 5. Thermodynamically aqueous (white region) and solid (brown region) As speciation with R1 in the anoxic (a) and oxic cycle (b) ($\Sigma As = 50 \times 10^{-6}$ and $\Sigma S = 100 \times 10^{-6}$) (M) and R2 in the anoxic (c) and oxic cycle (d) ($\Sigma As = 50 \times 10^{-6}$ and $\Sigma S = 1000 \times 10^{-6}$) (M) using PHREEQC code. The blue vertical areas represent pH values of the cycling experiments. (For interpretation of the references to colour in this figure legend, the reader is referred to the web version of this article.)

expected to be dominated by As(III), MTA(V), TTA(V), and TeTA (V) both at low (R1) and high (R2) sulfate contents (Fig. 5). Bath experiments revealed a mix of O-bound As(III) and As(V) species, with a ratio of As(III)/As(V) considerably increasing during the reducing half-cycles, and higher O-bound As(III) content than O-bound As (V) one, was observed in the last anoxic half-cycles, probably due to the enrichment of thioarsenate on $FeS_{2(s)}$ (Fig. 4, Table 3). However, the mechanism of thioarsenate sequestration in the Fe-As-S system requires further investigation to be confirmed, e.g. by performing EXAFS analysis to reveal the coordination of O-bound As(III) on Fe sulfides (e.g. $FeS_{(s)}$, $FeS_{2(s)}$) at low aqueous As concentrations. The fact that during anoxic half-cycles, the proportion of O-bound As(III) increases, and that aqueous As is removed during anoxic cycles could be due to the formation of aqueous thioarsenate sorbed on FeS_2. This would explain the observed increment of the O-bound As(III) species during the last anoxic half-cycles.

5. Conclusion

This study was aimed to better understand whether the high As concentrations detected in the aquifer in An Giang (Vietnam) can be attributed to redox dynamics. It has been shown that S and Fe biogeochemistry play a key role in determining the fate of As in deltaic sediments during redox oscillations. In particular, the results of this study indicate that: (i) As is first released during Fe reducing conditions but is then sequestered during SO_4^{2-} reduction; (ii) As adsorbs/desorbs on Fe-(oxyhydr)oxides, (iii) aqueous thioarsenic can form and be adsorbed on Fe sulfide minerals (e.g. FeS_2); and (iv) the reactions leading to the decrease of aqueous As concentrations over subsequent cycles are driven by microbial activity, which induces fermentation during anoxic periods, and respiratory consumption during oxic ones. While previous studies have shown that As mobility is controlled by reductive

dissolution of Fe-(oxyhydr)oxides in the reducing cycles, the results of the present work suggests that As sequestration in seasonally saturated sediments in the Mekong Delta Vietnam is controlled by the combined impact of surface hydrology, and by the reaction of Fe sulfide minerals and soluble As compounds (e.g. thioarsenic). This mechanism requires further investigation, e.g. by using techniques able to reveal the coordination of O-bound As(III) species on FeS_2, such as As K-edge EXAFS analysis.

Appendix A. Supplementary data

Supplementary data to this article can be found online at https://doi.org/10.1016/j.scitotenv.2019.01.219.

References

Allen, H.E., Fu, G., Deng, B., 1993. Analysis of acid-volatile sulfide (AVS) and simultaneously extracted metals (SEM) for the estimation of potential toxicity in aquatic sediments. Environ. Toxicol. Chem. 12, 1441–1453.

Anawar, H.M., Akai, J., Komaki, K., Terao, H., 2003. Geochemical occurrence of arsenic in groundwater of Bangladesh: sources and mobilization processes. J. Geochem. Explor. 77, 109–131. https://doi.org/10.1016/S0375-6742(02)00273-X.

Barton, L.L., 1995. In: Atkinson, T., Sherwood, R.F. (Eds.), Biotechnology Handbooks 8 - Sulfate-reducing Bacteria. Springer Science.

Benner, S.G., Polizzotto, M.L., Kocar, B.D., Ganguly, S., Phan, K., Ouch, K., Sampson, M., Fendorf, S., 2008. Groundwater flow in an arsenic-contaminated aquifer, Mekong Delta, Cambodia. Appl. Geochem. 23 (11), 3072–3087. https://doi.org/10.1016/j.apgeochem.2008.06.013.

Berg, M., Stengel, C., Pham, T.K.T., Pham, H.V., Sampson, M.L., Leng, M., Samreth, S., Fredericks, D., 2007. Magnitude of arsenic pollution in the Mekong and Red River Deltas - Cambodia and Vietnam. Sci. Total Environ. 372, 413–425. https://doi.org/10.1016/j.scitotenv.2006.09.010.

Berner, R.A., 1970. Sedimentary pyrite formation. Am. J. Sci. 268, 1–23.

Bohari, Y., Astruc, A., Astruc, M., Cloud, J., Angot, A.P., 2001. Improvements of hydride generation for the speciation of arsenic in natural freshwater samples by HPLC-HG-AFS. Anal. Atom. Spectrom. 16, 774–778. https://doi.org/10.1039/b101591p.

Bostick, B.C., Fendorf, S., 2003. Arsenite sorption on troilite (FeS) and pyrite (FeS2). Geochim. Cosmochim. Acta 67 (5), 909–921. https://doi.org/10.1016/S0016-7037(02)01170-5.

Burton, E.D., Sullivan, L.A., Bush, R.T., Johnston, S.G., Keene, A.F., 2008. A simple and inexpensive chromium-reducible sulfur method for acid-sulfate soils. Appl. Geochem. 23 (9), 2759–2766. https://doi.org/10.1016/j.apgeochem.2008.07.007.

Burton, Edward D., Johnston, Scott G., Planer-Friedrich, Britta, 2013. Coupling of arsenic mobility to sulfur transformations during microbial sulfate reduction in the presence and absence of humic acid. Chem. Geol. 343, 12–24.

Burton, E.D., Johnston, S.G., Kocar, B.D., 2014. Arsenic mobility during flooding of contaminated soil: the effect of microbial sulfate reduction. Environ. Sci. Technol. 48, 13660–13667.

Buschmann, J., Berg, M., 2009. Impact of sulfate reduction on the scale of arsenic contamination in groundwater of the Mekong, Bengal and Red River deltas. Appl. Geochem. 24 (7), 1278–1286. https://doi.org/10.1016/j.apgeochem.2009.04.002.

Buschmann, J., Berg, M., Stengel, C., Winkel, L., Sampson, M.L., Trang, P.T.K., Viet, P.H., 2008. Contamination of drinking water resources in the Mekong delta floodplains: arsenic and other trace metals pose serious health risks to population. Environ. Int. 34 (6), 756–764. https://doi.org/10.1016/j.envint.2007.12.025.

Caccavo, F., Lonergan, D.J., Lovley, D.R., Mark, D., Stolz, J.F., McInerney, M.J., 1994. Geobacter sulfurreducens sp. nov, a hydrogen- and acetate-oxidizing dissimilatory metal-reducing microorganism. Appl. Environ. Microbiol. 60 (10), 3752–3759.

Charlet, L., Morin, G., Rose, J., Wang, Y., Auffan, M., Burnol, A., Fernandez-Martinez, A., 2011. Reactivity at (nano)particle-water interfaces, redox processes, and arsenic transport in the environment. Compt. Rendus Geosci. 343, 123–139. https://doi.org/10.1016/j.crte.2010.11.005.

Cline, J.D., 1969. Spectrophotometric determination of hydrogen sulfide in natural waters. Limnol. Oceanogr. 14 (3), 454–458. https://doi.org/10.4319/lo.1969.14.3.0454.

Cotten, J., Le Dez, A., Bau, M., Caroff, M., Maury, R.C., Dulski, P., Fourcade, S., Bohn, M., Brousse, R., 1995. Origin of anomalous rare-earth element and yttrium enrichments in subaerially exposed basalts: evidence from French Polynesia. Chem. Geol. 119, 115–138. https://doi.org/10.1016/0009-2541(94)00102-E.

Couture, R.-M., Wallschläger, D., Rose, J., Van Cappellen, P., 2013a. Arsenic binding to organic and inorganic sulfur species during microbial sulfate reduction: a sediment flow-through reactor experiment. Environ. Chem. 10 (4), 285–294. https://doi.org/10.1071/EN13010.

Couture, R.-M.M., Rose, J., Kumar, N., Mitchell, K., Wallschläger, D., Van Cappellen, P., ... Van Cappellen, P., 2013b. Sorption of arsenite, arsenate, and thioarsenates to iron oxides and iron sulfides: a kinetic and spectroscopic investigation. Environ. Sci. Technol. 47 (11), 5652–5659. https://doi.org/10.1021/es3049724.

Couture, R.M., Charlet, L., Markelova, E., Madé, B., Parsons, C.T., 2015. On–off mobilization of contaminants in soils during redox oscillations. Environ. Sci. Technol. 49, 3015–3023. https://doi.org/10.1021/es5061879.

Couture, R.M., Fischer, R., Van Cappellen, P., Gobeil, C., 2016. Non-steady state diagenesis of organic and inorganic sulfur in lake sediments. Geochim. Cosmochim. Acta 194, 15–33. https://doi.org/10.1016/j.gca.2016.08.029.

Cypionka, H., 2001. Periplasmic oxygen reduction by Desulfovibrio species. Arch. Microbiol. 176, 306–309. https://doi.org/10.1007/s002030100329.

Cytryn, E., Minz, D., Gelfand, I., Neori, A., Gieseke, A., De Beer, D., Van Rijn, J., 2005. Sulfide-oxidizing activity and bacterial community structure in a fluidized bed reactor from a zero-discharge mariculture system. Environ. Sci. Technol. 39 (6), 1802–1810.

Dobbin, P.S., Carter, J.P., San Juan, C.G., von Hobe, M., Powell, A.K., Richardson, D.J., 1999. Dissimilatory Fe(III) reduction by Clostridium beijerinckii isolated from freshwater sediment using Fe(III) maltol enrichment. FEMS Microbiol. Lett. 176, 131–138.

Van Dongen, B.E., Rowland, H.A.L., Gault, A.G., Polya, D.A., Bryant, C., Pancost, R.D., 2008. Hopane, sterane and n-alkane distributions in shallow sediments hosting high arsenic groundwaters in Cambodia. Appl. Geochem. 23, 3047–3058. https://doi.org/10.1016/j.apgeochem.2008.06.012.

Edgar, R.C., 2013. UPARSE: highly accurate OTU sequences from microbial amplicon reads. Nat. Methods 10 (10), 996–998. https://doi.org/10.1038/nmeth.2604.

Edgar, Robert C., Haas, Brian J., Clemente, Jose C., Quince, Christopher, Knight, Rob, 2011. UCHIME improves sensitivity and speed of chimera detection. Bioinformatics 27 (16), 2194–2200. https://doi.org/10.1093/bioinformatics/btr381.

Eller, G., Frenzel, P., 2001. Changes in activity and community structure of methane-oxidizing bacteria over the growth period of rice. Appl. Environ. Microbiol. 67 (6), 2395–2403. https://doi.org/10.1128/AEM.67.6.2395.

Erban, L.E., Gorelick, S.M., Zebker, H. a, Fendorf, S., 2013. Release of arsenic to deep groundwater in the Mekong Delta, Vietnam, linked to pumping-induced land subsidence. Proc. Natl. Acad. Sci. U. S. A. 110 (34), 13751–13756. https://doi.org/10.1073/pnas.1300503110.

Essington, M., 2004. Soil and Water Chemistry an Integrative Approach. CRC Press, Boca Raton.

Fan, L., McElroy, K., Thomas, T., 2012. Reconstruction of ribosomal RNA genes from metagenomic data. PLoS ONE 7 (6). https://doi.org/10.1371/journal.pone.0039948.

Fendorf, S., Nico, P.S., Kocar, B.D., Yoko, M., Tufano, K.J., 2010. Arsenic Chemistry in Soils and Sediments. Lawrence Berkeley National Laboratory.

Franciscon, E., Zille, A., Fantinatti-Garboggini, F., Silva, I.S., Cavaco-Paulo, A., Durrant, L.R., 2009. Microaerophilic-aerobic sequential decolourization/biodegradation of textile azo dyes by a facultative Klebsiella sp. strain VN-31. Process Biochem. 44 (4), 446–452. https://doi.org/10.1016/j.procbio.2008.12.009.

Graff, A., Stubner, S., 2003. Isolation and molecular characterization of thiosulfate-oxidizing bacteria from an Italian rice field soil. Syst. Appl. Microbiol. 26, 445–452. https://doi.org/10.1078/072320203322497482.

Hanh, H.T., Kim, K.W., Bang, S., Hoa, N.M., 2011. Community exposure to arsenic in the Mekong river delta, Southern Vietnam. J. Environ. Monit. 13 (7), 2025–2032. https://doi.org/10.1039/c1em10037h.

Harvey, C.F., Swartz, C.H., Badruzzaman, A.B.M., Keon-Blute, N., Yu, W., Ali, M.A., ... Ahmed, M.F., 2002. Arsenic mobility and groundwater extraction in Bangladesh. Science 298, 1602–1606. https://doi.org/10.1126/science.1076978.

He, J., Charlet, L., 2013. A review of arsenic presence in China drinking water. J. Hydrol. 492, 79–88. https://doi.org/10.1016/j.jhydrol.2013.04.007.

Hedrich, S., Schlomann, M., Barrie Johnson, D., 2011a. The iron-oxidizing proteobacteria. Microbiology 157 (6), 1551–1564. https://doi.org/10.1099/mic.0.045344-0.

Hedrich, S., Schlomann, M., Johnson, D.S., 2011b. The iron-oxidizing proteobacteria. Microbiology 157, 1551–1564.

Helz, G.R., Tossell, J.A., 2008. Thermodynamic model for arsenic speciation in sulfidic waters: a novel use of ab initio computations. Geochim. Cosmochim. Acta 72, 4457–4468. https://doi.org/10.1016/j.gca.2008.06.018.

Héry, M., Gault, A.G., Rowland, H.A.L., Lear, G., Polya, D.A., Lloyd, J.R., 2008. Molecular and cultivation-dependent analysis of metal-reducing bacteria implicated in arsenic mobilisation in South-East Asian aquifers. Appl. Geochem. 23, 3215–3223. https://doi.org/10.1016/j.apgeochem.2008.07.003.

Héry, M., Rizoulis, A., Sanguin, H., Cooke, D.A., Pancost, R.D., Polya, D.A., Lloyd, J.R., 2015. Microbial ecology of arsenic-mobilizing Cambodian sediments: lithological controls uncovered by stable-isotope probing. Environ. Microbiol. 17 (6), 1857–1869. https://doi.org/10.1111/1462-2920.12412.

Hoang, T.H., Bang, S., Kim, K.-W., Nguyen, M.H., Dang, D.M., 2010. Arsenic in groundwater and sediment in the Mekong River delta, Vietnam. Environ. Pollut. 158, 2648–2658. https://doi.org/10.1016/j.envpol.2010.05.001.

Hohmann, C., Morin, G., Ona-nguema, G., Guigner, J., Brown, G.E., Kappler, A., 2011. Molecular-level modes of As binding to Fe (III) (oxyhydr) oxides precipitated by the anaerobic nitrate-reducing Fe(II)-oxidizing Acidovorax sp. strain BoFeN1. Geochim. Cosmochim. Acta 75, 4699–4712. https://doi.org/10.1016/j.gca.2011.02.044.

Holmes, Dawn E., Nevin, Kelly P., Woodard, Trevor L., Peacock, Aaron D., Lovley, Derek R., 2007. Prolixibacter bellariivorans gen. nov., sp. nov., a sugar-fermenting, psychrotolerant anaerobe of the phylum Bacteroidetes, isolated from a marine-sediment fuel cell. Int. J. Syst. Evol. Microbiol. 57, 701–707.

Hoque, M.A., Khan, A.A., Shamsudduha, M., Hossain, M.S., Islam, T., Chowdhury, S.H., 2009. Near surface lithology and spatial variation of arsenic in the shallow groundwater: Southeastern Bangladesh. Environ. Geol. 56 (8), 1687–1695. https://doi.org/10.1007/s00254-008-1267-3.

Horneman, A., van Geen, A., Kent, D.V., Mathe, P.E., Zheng, Y., Dhar, R.K., ... Ahmed, K.M., 2004. Decoupling of As and Fe release to Bangladesh groundwater under reducing conditions. Part I: evidence from sediment profiles. Geochim. Cosmochim. Acta 68 (17), 3459–3473. https://doi.org/10.1016/j.gca.2004.01.026.

Hsieh, Y.P., Chung, S.W., Tsau, Y.J., Sue, C.T., 2002. Analysis of sulfides in the presence of ferric minerals by diffusion methods. Chem. Geol. 182 (2–4), 195–201. https://doi.org/10.1016/S0009-2541(01)00282-0.

Hurtgen, M.T., Lyons, T.W., Ingall, E.D., Cruse, A.M., 1999. Anomalous enrichments of iron monosulfide in euxinic marine sediments and the role of H2S in iron sulfide transformations: examples from Effingham inlet, Orca Basin, and the Black Sea. Am. J. Sci. 299, 556–588.

Karimian, N., Johnston, S.G., Burton, E.D., 2017. Effect of cyclic redox oscillations on water quality in freshwater acid sulfate soil wetlands. Sci. Total Environ. 581–582, 314–327. https://doi.org/10.1016/j.scitotenv.2016.12.131.

Kocar, B.D., Fendorf, S., 2012. Arsenic release and transport in sediments of the Mekong Delta. Environmental Pollution and Ecotoxicology, pp. 117–124.

Kocar, B.D., Polizzotto, M.L., Benner, S.G., Ying, S.C., Ung, M., Ouch, K., ... Fendorf, S., 2008. Integrated biogeochemical and hydrologic processes driving arsenic release from shallow sediments to groundwaters of the Mekong delta. Appl. Geochem. 23 (11), 3059–3071. https://doi.org/10.1016/j.apgeochem.2008.06.026.

Kumaresan, D., Wischer, D., Hillebrand-Voiculescu, A., Murrell, J.C., 2015. Draft genome sequences of facultative Methylotrophs, Gemmobacter sp. strain LW1 and Mesorhizobium sp. strain 1M-11, isolated from Movile cave, Romania. Genome Announc. 3 (6), 2015.

Langner, P., Mikutta, C., Kretzschmar, R., 2012. Arsenic sequestration by organic sulphur in peat. Nat. Geosci. 5, 66–73. https://doi.org/10.1038/ngeo1329.

Langner, P., Mikutta, C., Suess, E., Marcus, M.A., Kretzschmar, R., 2013. Spatial distribution and speciation of arsenic in peat studied with microfocused X-ray fluorescence spectrometry and X-ray absorption spectroscopy. Environ. Sci. Technol. 47, 9706–9714.

Lawson, M., Polya, D.A., Boyce, A.J., Bryant, C., Mondal, D., Shantz, A., Ballentine, C.J., 2013. Pond-derived organic carbon driving changes in arsenic hazard found in Asian groundwaters. Environ. Sci. Technol. 47 (13), 7085–7094.

Lawson, M., Polya, D.A., Boyce, A.J., Bryant, C., Ballentine, C.J., 2016. Tracing organic matter composition and distribution and its role on arsenic release in shallow Cambodian groundwaters. Geochim. Cosmochim. Acta 178, 160–177. https://doi.org/10.1016/j.gca.2016.01.010.

Le Pape, P., Blanchard, M., Brest, J., Boulliard, J., Ikogou, M., Stetten, L., ... Morin, G., 2017. Arsenic incorporation in pyrite at ambient temperature at both tetrahedral S−I and octahedral FeII sites: evidence from EXAFS−DFT analysis. Environ. Sci. Technol. 51, 150–158. https://doi.org/10.1021/acs.est.6b03502.

Lear, G., Song, B., Gault, A.G., Polya, D.A., Lloyd, J.R., 2007. Molecular analysis of arsenate-reducing bacteria within Cambodian sediments following amendment with acetate. Appl. Environ. Microbiol. 73 (4), 1041–1048. https://doi.org/10.1128/AEM.01654-06.

Li, H., Peng, J., Weber, K.A., Zhu, Y., 2011. Phylogenetic diversity of Fe (III)-reducing microorganisms in rice paddy soil: enrichment cultures with different short-chain fatty acids as electron donors. J. Soils Sediment 11, 1234–1242.

Lin, W.C., Coppi, M.V., Lovley, D.R., 2004. Geobacter sulfurreducens can grow with oxygen as a terminal electron acceptor. Appl. Environ. Microbiol. 70 (4), 2525–2528. https://doi.org/10.1128/AEM.70.4.2525.

Lovley, D.R., Phillips, E.J.P., 1986. Organic matter mineralization with reduction of ferric iron in anaerobic sediments. Appl. Environ. Microbiol. 51 (4), 683–689.

Luan, H.H., Medzhitov, R., 2016. Food fight: role of itaconate and other metabolites in antimicrobial defense. Cell Metab. 24, 379–387. https://doi.org/10.1016/j.cmet.2016.08.013.

Lynd, L.R., Weimer, P.J., Willem, H. van Z., Isak, P.S., 2002. Microbial cellulose utilization: fundamentals and biotechnology. Microbiol. Mol. Biol. Rev. 66 (3), 506–577. https://doi.org/10.1128/MMBR.66.3.506.

Magnone, D., Richards, L.A., Polya, D.A., Bryant, C., Jones, M., Van Dongen, B.E., 2017. Biomarker-indicated extent of oxidation of plant-derived organic carbon (OC) in relation to geomorphology in an arsenic contaminated Holocene aquifer, Cambodia. Sci. Rep. 7, 1–12. https://doi.org/10.1038/s41598-017-13354-8 (Art. 13093).

Markelova, E., Couture, R.-M., Parsons, C.T., Markelov, I., Madé, B., Van Cappellen, P., Charlet, L., 2018. Speciation dynamics of oxyanion contaminants (As, Sb, Cr) in argillaceous suspensions during oxic-anoxic cycles. Appl. Geochem. https://doi.org/10.1016/j.apgeochem.2017.12.012.

McGuire, M.M., Hamers, R.J., 2000. Extraction and quantitative analysis of elemental sulfur from sulfide mineral surfaces by high-performance liquid chromatography. Environ. Sci. Technol. 34 (21), 4651–4655. https://doi.org/10.1021/es0011663.

Métral, J., Charlet, L., Bureau, S., Mallik, S.B., Chakraborty, S., Ahmed, K.M., ... Van Geen, A., 2008. Comparison of dissolved and particulate arsenic distributions in shallow aquifers of Chakdaha, India, and Araihazar, Bangladesh. Geochem. Trans. 9 (1), 1. https://doi.org/10.1186/1467-4866-9-1.

Miot, J., Morin, G., Skouri-Paner, F., Férard, C., Aubry, E., Briand, J., ... Brown, G.E., 2008. XAS study of arsenic coordination in Euglena gracilis exposed to arsenite. Environ. Sci. Technol. 42, 5342–5347.

Muyzer, G., Stams, A.J.M., 2008. The ecology and biotechnology of sulphate-reducing bacteria. Nat. Rev. Microbiol. 6 (6), 441–454. https://doi.org/10.1038/nrmicro1892.

Neumann, T., Leipe, T., Shimmield, G., 1998. Heavy metal enriched surficial sediments in the Oder River discharge area: source or sink for heavy metals? Appl. Geochem. 13, 329–337.

Nguyen, K.P., Itoi, R., 2009. Source and release mechanism of arsenic in aquifers of the Mekong Delta, Vietnam. J. Contam. Hydrol. 103, 58–69. https://doi.org/10.1016/j.jconhyd.2008.09.005.

Nguyen, V.L., Ta, T.K.O., Tateishi, M., 2000. Late Holocene depositional environments and coastal evolution of the Mekong River Delta, Southern Vietnam. J. Asian Earth Sci. 18 (4), 427–439. https://doi.org/10.1016/S1367-9120(99)00076-0.

Nguyen, T.P., Helbling, D.E., Bers, K., Fida, T.T., Wattiez, R., Kohler, H.P., Springael, D., De Mot, R., 2014. Genetic and metabolic analysis of the carbofuran catabolic pathway in Novosphingobium sp. KN65.2. Appl. Microbiol. Biotechnol. 98 (19), 8235–8252. https://doi.org/10.1007/s00253-014-5858-5.

Nickson, R.T., Mcarthur, J.M., Ravenscroft, P., Burgess, W.G., Ahmed, K.M., 2000. Mechanism of arsenic release to groundwater, Bangladesh and West Bengal. Appl. Geochem. 15 (4), 403–413. https://doi.org/10.1016/S0883-2927(99)00086-4.

O'Day, P.A., Vlassopoulos, D., Root, R., Rivera, N., 2004. The influence of sulfur and iron on dissolved arsenic concentrations in the shallow subsurface under changing redox conditions. Proc. Natl. Acad. Sci. U. S. A. 101 (38), 13703–13708. https://doi.org/10.1073/pnas.0402775101.

Ona-Nguema, G., Morin, G., Juillot, F., Calas, G., Brown Jr., G.E., 2005. EXAFS analysis of arsenite adsorption onto two-line ferrihydrite, hematite, goethite, and lepidocrocite. Environ. Sci. Technol. 39, 9147–9155.

Parkhurst, D.L., Appelo, C.A.J., 2013. Description of input and examples for PHREEQC version 3 - a computer program for speciation, batch-reaction, one-dimensional transport, and inverse geochemical calculations. U.S. Geological Survey Techniques and Methods https://doi.org/10.1016/0029-6554(94)90020-5.

Parsons, C.T., Couture, R.-M., Omoregie, E.O., Bardelli, F., Greneche, J.-M., Roman-Ross, G., Charlet, L., 2013. The impact of oscillating redox conditions: arsenic immobilisation in contaminated calcareous floodplain soils. Environ. Pollut. 178, 254–263. https://doi.org/10.1016/j.envpol.2013.02.028.

Phan, V.T.H., Bardelli, F., Le, P., Couture, R., Fernandez-martinez, A., Tisserand, D., et al., 2018. Interplay of S and As in Mekong Delta sediments during redox oscillations. Geosci. Front. https://doi.org/10.1016/j.gsf.2018.03.008.

Van Phan, T.H., Bonnet, T., Garambois, S., Tisserand, D., Bardelli, F., Bernier-Latmani, R., Charlet, L., 2017. Arsenic in shallow aquifers linked to the electrical ground conductivity: the Mekong Delta source example. Geosci. Res. 2 (3), 180–195.

Pokorna, D., Zabranska, J., 2015. Sulfur-oxidizing bacteria in environmental technology. Biotechnol. Adv. 33, 1246–1259.

Polizzotto, M.L., Harvey, C.F., Sutton, S.R., Fendorf, S., 2005. Processes conducive to the release and transport of arsenic into aquifers of Bangladesh. Proc. Natl. Acad. Sci. 102 (52), 18819–18823.

Polizzotto, M.L., Kocar, B.D., Benner, S.G., Sampson, M., Fendorf, S., 2008. Near-surface wetland sediments as a source of arsenic release to ground water in Asia. Nature 454 (7203), 505–508. https://doi.org/10.1038/nature07093.

Polya, D.A., Gault, A.G., Diebe, N., Feldman, P., Rosenboom, J.W., Gilligan, E., ... Cooke, D.A., 2005. Arsenic hazard in shallow Cambodian groundwaters. Mineral. Mag. 69 (5), 807–823. https://doi.org/10.1180/0026461056950290.

Poulain, A.J., Newman, D.K., 2009. Rhodobacter capsulatus catalyzes light-dependent Fe (II) oxidation under anaerobic conditions as a potential detoxification mechanism. Appl. Environ. Microbiol. 75 (21), 6639–6646. https://doi.org/10.1128/AEM.00054-09.

Poulton, S.W., Krom, M.D., Raiswell, R., 2004. A revised scheme for the reactivity of iron (oxyhydr)oxide minerals towards dissolved sulfide. Geochim. Cosmochim. Acta 68, 3703–3715.

Raiswell, R., Berner, R.A., 1985. Pyrite formation in euxinic and semi-euxinic sediments. Am. J. Sci. https://doi.org/10.2475/ajs.285.8.710.

Ravel, B., Newville, M., 2005. Athena, Artemis, Hephaestus: data analysis for X-ray absorption spectroscopy using Ifeffit. J. Synchrotron Radiat. 12 (4), 537–541. https://doi.org/10.1107/S0909049505012719.

Resongles, E., Pape, P., Morin, G., Delpoux, S., Brest, J., Guo, S., Casiot, C., 2016. Routine determination of inorganic arsenic speciation in precipitates from acid mine drainage using orthophosphoric acid extraction. Anal. Methods 8, 7420–7426. https://doi.org/10.1039/C6AY02084D.

Rickard, D., 2006. The solubility of FeS. Geochim. Cosmochim. Acta 70 (23), 5779–5789. https://doi.org/10.1016/j.gca.2006.02.029.

Rickard, D., Iii, G.W.L., 2007. Chemistry of iron sulfides. Chem. Rev. 44, 514–562.

Rickard, D., Morse, J.W., 2005. Acid volatile sulfide (AVS). Mar. Chem. 97, 141–197. https://doi.org/10.1016/j.marchem.2005.08.004.

Rittle, Keith A., Drever, James I., Colberg, Patricia J.S., 1995. Precipitation of arsenic during bacterial sulfate reduction. Geomicrobiol J. 13 (1), 1–11. https://doi.org/10.1080/01490459509378000.

Rizoulis, A., Al Lawati, W.M., Pancost, R.D., Polya, D.A., Van Dongen, B.E., Lloyd, J.R., 2014. Microbially mediated reduction of Fe(III) and As(V) in Cambodian sediments amended with 13C-labelled hexadecane and kerogen. Environ. Chem. 11, 538–546. https://doi.org/10.1071/EN13238.

Rochette, E.A., Bostick, B.C., Li, G., Fendorf, S., 2000. Kinetics of arsenate reduction by dissolved sulfide. Environ. Sci. Technol. 34 (22), 4714–4720. https://doi.org/10.1021/es000963y.

Root, R.A., Dixit, S., Campbell, K.M., Jew, A.D., Hering, J.G., O'Day, P.A., 2007. Arsenic sequestration by sorption processes in high-iron sediments. Geochim. Cosmochim. Acta 71, 5782–5803. https://doi.org/10.1016/j.gca.2007.04.038.

Root, R.A., Vlassopoulos, D., Rivera, N.A., Rafferty, M.T., Andrews, C., O'Day, P.A., 2009. Speciation and natural attenuation of arsenic and iron in a tidally influenced shallow aquifer. Geochim. Cosmochim. Acta 73 (19), 5528–5553. https://doi.org/10.1016/j.gca.2009.06.025.

Rowland, H.A.L., Pederick, R.L., Polya, D.A., Pancost, R.D., van Dongen, B.E., Gault, A.G., ... Lloyd, J.R., 2007. The control of organic matter on microbially mediated iron reduction and arsenic release in shallow alluvial aquifers. Geobiology 5, 281–292. https://doi.org/10.1111/j.1472-4669.2007.00100.x.

Schellenberger, S., Drake, H.L., Kolb, S., 2011. Functionally redundant cellobiose-degrading soil bacteria respond differentially to oxygen. Appl. Environ. Microbiol. 77 (17), 6043–6048. https://doi.org/10.1128/AEM.00564-11.

Schmeisser, C., Liesegang, H., Krysciak, D., Bakkou, N., Le Quéré, A., Wollherr, A., Heinemeyer, I., Morgenstern, B., Pommerening-Röser, A., Flores, M., Palacios, R., Brenner, S., Gottschalk, G., Schmitz, R.A., Broughton, W.J., Perret, X., Strittmatter, A.W., Streit, W.R., 2009 Jun. Rhizobium sp. strain NGR234 possesses a remarkable number of secretion systems. Appl. Environ. Microbiol. 75 (12), 4035–4045. https://doi.org/10.1128/AEM.00515-09.

Schwedt, G., Rieckhoff, M., 1996. Separation of thio- and oxothioarsenates by capillary zone electrophoresis and ion chromatography. J. Chromatogr. A 736, 341–350. https://doi.org/10.1016/0021-9673(95)01319-9.

Snoeyenbos-West, O.L., Nevin, K.P., Anderson, R.T., Lovley, D.R., 2000. Enrichment of Geobacter species in response to stimulation of Fe(III) reduction in sandy aquifer sediments. Microb. Ecol. 39, 153. https://doi.org/10.1007/s002480000018.

Stookey, L.L., 1970. Ferrozine—a new spectrophotometric reagent for iron. Anal. Chem. 42 (7), 779–781. https://doi.org/10.1021/ac60289a016.

Stuckey, J.W., Schaefer, M.V., Kocar, B.D., Dittmar, J., Lezama, J., Benner, S.G., Fendorf, S., 2015. Peat formation concentrates arsenic within sediment deposits of the Mekong Delta. Geochim. Cosmochim. Acta 149, 190–205. https://doi.org/10.1016/j.gca.2014.10.021.

Stuckey, J.W., Schaefer, M.V., Kocar, B.D., Benner, S.G., Fendorf, S., 2016. Arsenic release metabolically limited to permanently water-saturated soil in Mekong Delta. Nat. Geosci. 9, 70–76. https://doi.org/10.1038/NGEO2589.

Suess, E., Scheinost, A.C., Bostick, B.C., Merkel, B.J., Wallschlaeger, D., Planer-Friedrich, B., 2009. Discrimination of thioarsenites and thioarsenates by X-ray absorption spectroscopy. Anal. Chem. 81 (20), 8318–8326. https://doi.org/10.1021/ac901094b.

Tang, K., Baskaran, V., Nemati, M., 2009. Bacteria of the sulphur cycle: an overview of microbiology, biokinetics and their role in petroleum and mining industries. 44, 73–94.

Thabet, O.B.D., Fardeau, M.-L., Joulian, C., et al., 2004. *Clostridium tunisiense* sp. nov., a new proteolytic, sulfur-reducing bacterium isolated from an olive mill wastewater contaminated by phosphogypse Anaerobe. 10, 185–190. https://doi.org/10.1016/j.anaerobe.2004.04.002.

Thomasarrigo, L.K., Mikutta, C., Lohmayer, R., Planer-friedrich, B., Kretzschmar, R., 2016. Sulfidization of organic freshwater flocs from a minerotrophic peatland: speciation changes of iron, sulfur, and arsenic. Environ. Sci. Technol. 50 (7), 3607–3616. https://doi.org/10.1021/acs.est.5b05791.

Thompson, A., Chadwick, O.A., Rancourt, D.G., Chorover, J., 2006. Iron-oxide crystallinity increases during soil redox oscillations. Geochim. Cosmochim. Acta 70 (7), 1710–1727. https://doi.org/10.1016/j.gca.2005.12.005.

Van Geen, A., Zheng, Y., Stute, M., Ahmed, K.M., 2003. Comment on "Arsenic mobility and groundwater extraction in Bangladesh" (II). Science 300, 584. https://doi.org/10.1126/science.1081057.

Van Geen, A., Radloff, K., Aziz, Z., Cheng, Z., Huq, M.R., Ahmed, K.M., ... Upreti, B.N., 2008. Comparison of arsenic concentrations in simultaneously-collected groundwater and aquifer particles from Bangladesh, India, Vietnam, and Nepal. Appl. Geochem. 23 (11), 3019–3028. https://doi.org/10.1016/j.apgeochem.2008.07.005.

Viollier, E., Inglett, P.W., Hunter, K., Roychoudhury, A.N., Van Cappellen, P., 2000. The ferrozine method revisited: Fe(II)/Fe(III) determination in natural waters. Appl. Geochem. 15 (6), 785–790. https://doi.org/10.1016/S0883-2927(99)00097-9.

Wan, M., Shchukarev, A., Lohmayer, R., Planer-friedrich, B., Pei, S., 2014. Occurrence of surface polysulfides during the interaction between ferric (hydr)oxides and aqueous sulfide. Environ. Sci. Technol. 48 (9), 5076–5084.

Wang, Y., Sheng, H., He, Y., Wu, J., Jiang, Y., Tam, N.F., Zhou, H., 2012. Comparison of the levels of bacterial diversity in freshwater, intertidal wetland, and marine sediments by using millions of AEM. 78 (23), 8264–8271. https://doi.org/10.1128/AEM.01821-12.

Wang, Y., Le Pape, P., Morin, G., Asta, M., King, G., Bartova, B., ... Bernier-Latmani, R., 2018. Arsenic speciation in Mekong Delta sediments depends on their depositional environment. Environ. Sci. Technol. Lett. 52 (6), 3431–3439. https://doi.org/10.1021/acs.est.7b05177.

WHO, 2004. Some Drinking-water Disinfectants and Contaminants, Including Arsenic. vol. 83.

Willems, A., Gillis, M., 2015. In: Whitman, W.B., Rainey, F., Kämpfer, P., Trujillo, M., Chun, J., DeVos, P., Hedlund, B., Dedysh, S. (Eds.), *Acidovorax*. Bergey's manual of systematics of archaea and bacteria. https://doi.org/10.1002/9781118960608.gbm00943

Willems, A., Busse, J., Goor, M., Pot, B., Falsen, E., Jantzen, E., ... Gillis, M., 1989. Hydrogenophaga, a new genus of hydrogen-oxidizing bacteria that includes Hydrogenophaga flava comb. nov. (formerly Pseudomonas flava), Hydrogenophaga palleronii (formerly pseudomonas palleronii), Hydrogenophaga pseudoflava (formerly pseudomonas pseudofla). Int. J. Syst. Bacteriol. 39 (3), 319–333.

Winkel, L.H.E., Trang, P., Vi, L., Stengel, C., Amini, M., Nguyen, H., ... Berg, M., 2010. Arsenic pollution of groundwater in Vietnam exacerbated by deep aquifer exploitation for more than a century. PNAS 108 (4), 1246–1251. https://doi.org/10.1073/pnas.1011915108/.

Wirsen, C.O., Sievert, S.M., Cavanaugh, C.M., Molyneaux, S.J., Ahmad, A., Taylor, L.T., DeLong, E.F., Taylor, C.D., 2002. Characterization of an autotrophic sulfide-oxidizing marine arcobacter sp. that produces filamentous sulfur. Appl. Environ. Microbiol. 68 (1), 316–325. https://doi.org/10.1128/ aem.68.1.316-325.2002.

Wolterink, A., Kim, S., Muusse, M., Kim, I.S., Roholl, P.J.M., Van Ginkel, C.G., Stams, A.J.M., Kengen, S.W.M., 2005. *Dechloromonas hortensis* sp. nov. and strain ASK-1, two novel (per)chlorate-reducing bacteria, and taxonomic description of strain GR-1. Int. J. Syst. Evol. Microbiol. 55, 2063–2068.

Wolthers, M., Charlet, L., van Der Weijden, C.H., van der Linde, P.R., Rickard, D., 2005. Arsenic mobility in the ambient sulfidic environment: sorption of arsenic(V) and arsenic(III) onto disordered mackinawite. Geochim. Cosmochim. Acta 69 (14), 3483–3492. https://doi.org/10.1016/j.gca.2005.03.003.

Zhang, J., Kobert, K., Flouri, T., Stamatakis, A., 2014. PEAR: a fast and accurate Illumina paired-end reAd mergeR. Bioinformatics 30 (5), 614–620. https://doi.org/10.1093/bioinformatics/btt593.

Zheng, Y., Stute, M., Van Geen, A., Gavrieli, I., Dhar, R., 2004. Redox control of arsenic mobilization in Bangladesh groundwater. Appl. Geochem. 19, 201–214. https://doi.org/10.1016/j.apgeochem.2003.09.007.